Porous materials for low-temperature H_2S-removal in fuel cell applications

Donglai Mao[1], John M Griffin[2,3], Richard Dawson[1], Alasdair Fairhurst[4], Gaurav Gupta[1], Nuno Bimbo[1,†*]

[1]Department of Engineering, Lancaster University, Lancaster LA1 4YW, United Kingdom

[2]Department of Chemistry, Lancaster University, LA1 4YB, United Kingdom

[3]Materials Science Institute, Lancaster University, LA1 4YB, United Kingdom

[4]NanoSUN Limited, Lancaster, LA1 3NX, United Kingdom

[†]Present address: School of Chemistry, University of Southampton, Southampton, SO17 1BJ, United Kingdom

*Corresponding Author: n.bimbo@soton.ac.uk

ABSTRACT: When fuel gases (H_2 and CH_4) for fuel cells are produced from fossil fuels and biomass, there is a high possibility of presence of hydrogen sulfide (H_2S). Because H_2S can poison fuel cells and cause long lasting damage, it is necessary to rigorously remove H_2S from fuel gases before use in fuel cells. With the advantages of high efficiency and low energy consumption, desulphurisation via adsorption at low temperatures has attracted the attention of many researchers and has seen recent advances. This review compares the performance of commonly-studied porous materials (metal oxides, activated carbon, zeolites, silica, and metal-organic frameworks (MOF)) that are used for adsorption at low temperatures. Test conditions such as feed gas compositions, feed gas velocity, and breakthrough concentration threshold are considered when comparing the adsorption performance of the materials. High performing materials from each material category are identified and future research directions are discussed.

Keywords: Hydrogen sulfide, Adsorption, Activated Carbon, Mesoporous Silica, Metal-organic Frameworks

1. Introduction

With the increasing urgency of tackling global warming and climate change, many countries have agreed to take actions to reduce greenhouse gas emissions. In the EU, an 80 - 95% reduction in greenhouse gas emissions (compared to the 1990 levels) target has been set for 2050 [1]. Many new technologies have been proposed to mitigate greenhouse gas emissions and among these, fuel cells have been gaining attention lately. Fuel cells are electrochemical devices that utilise fuel gases and air to generate power via electrochemical reactions. When H_2 is used as the fuel gas, the only byproduct of the reaction is water. Compared to traditional combustion processes, they have the advantages of much higher efficiencies and cleaner processes. Hence, they are seen as a crucial element in reaching greenhouse gas emission reduction targets [1]. Commonly used fuel gases for fuel cells are H_2 and CH_4, depending on the type of fuel cell. For example, proton exchange membrane fuel cell (PEM) and alkaline fuel cell (AFC) can only use H_2 as fuel gas. By contrast, molten carbonate fuel cell (MCFC)

and solid oxide fuel cell (SOFC) can use both H_2 and CH_4 as their fuel gases [2]. Figure 1 shows typical compositions of H_2S in various gas sources for hydrogen production. After they are converted into hydrogen, the H_2S content can stay between a few ppm to more than 1% depending on the production methods [3-11]. Research has shown that even the existence of ppm levels of H_2S is enough to poison fuel cell components and cause irreversible damage [12-16]. The international standard for hydrogen fuel quality (ISO 14687) will be mandatory in the EU from November 2021 and currently states a maximum concentration limit of 0.004 ppmv for sulphur compounds [17]. With the potential damage caused by poisoning of fuel cells and particularly stringent legislative requirements, it is vital to thoroughly remove H_2S from fuel gases before use.

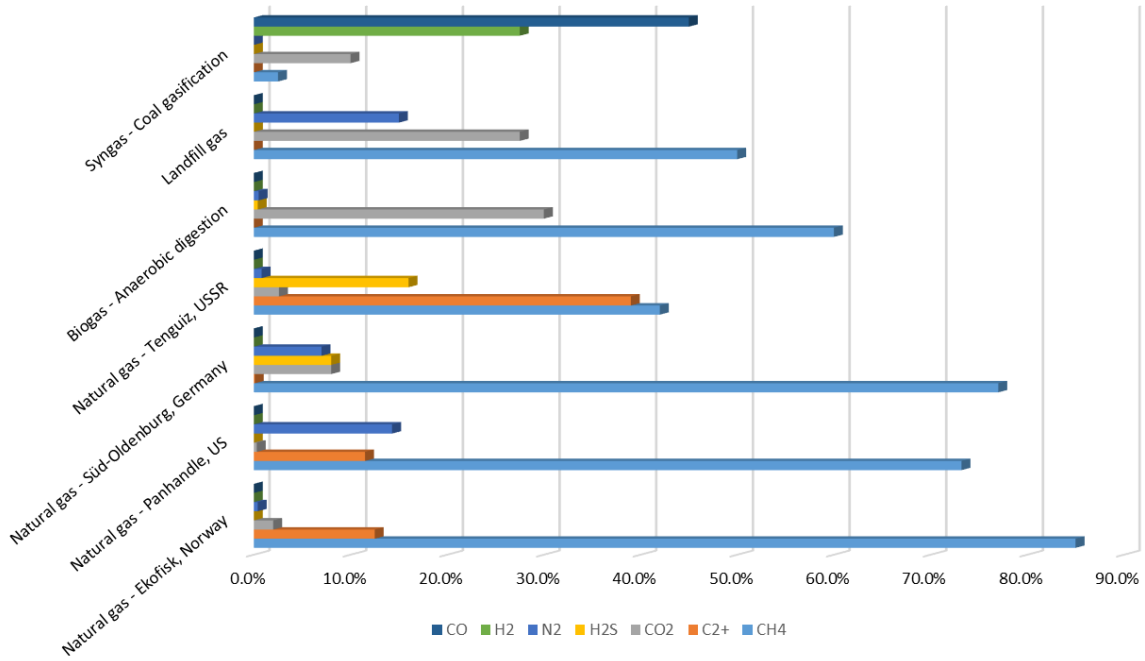

Figure 1. Compositions of raw H_2S-containing gases from different sources [11].

There have been many methods developed to remove sulphur from gas streams/fossil fuels, especially in industrial oil refineries. This includes hydrodesulphurisation, oxidative desulphurisation, biodesulphurisation, absorption, selective adsorption, and membrane separation among others [11, 17, 18]. In a commercial environment, the most commonly employed methods to remove sulphur from gases are absorption methods (e.g. amine scrubbing and physical solvent process). However, different methods have different pros and cons, affecting their suitability to be adopted for industrial applications. In addition, factors such as types of impurity gases, the content of sulphur in the feedstock, and stages of fuel processing should also be considered when selecting a desulphurisation method in practical applications. For example, the fossil fuel conversion stage normally uses hydrodesulphurisation or thermal

cracking methods to remove sulphur. By contrast, the finishing stage in a refinery normally employs methods such as absorption methods and membrane separation system to remove sulphur from gases. In addition, when the partial pressures of acid gases are low, amine scrubbing process can be very effective in removing the majority of sulphur from gases. When the partial pressures of acid gases are higher than 345 kPa, physical solvent absorption methods tend to be utilised. [18, 19].

With advantages such as high efficiency and low energy consumption, many researchers have been focusing on the study of desulphurisation using adsorbents at low temperatures during the last decade. Shah et al reviewed a wide range of separation technologies (absorption, adsorption, membranes, and cryogenic distillation) and materials that have been reported for H_2S removal. The materials summarised in the paper include liquid and solid compounds which were reported to remove H_2S from gases at either room temperatures or high temperatures [11]. Ahmad et al reviewed the progress of adsorbents derived from waste materials in biogas desulphurisation and concluded that further exploration is required for the commercialisation of the materials despite their great potential [20]. Khabazipour et al summarised porous materials that have been modified using different methods for H_2S removal at either room temperatures or high temperatures [21]. More review papers focusing on H_2S removal from different gas streams can also be found in the following references [22-25]. Despite the high number of review papers on H_2S removal with porous materials, past work generally focuses on reporting the progress that has been made for a given type of material following a timeline, modification technique, or different synthesis method. In addition, most combine the performance of a material in removing H_2S at both low temperatures (20-40 °C) and high temperatures (40-800 °C). With the vast difference in experimental conditions and adsorption capacity units, the performance of each material in removing H_2S has not yet been compared using a constant basis, and it is unclear which material is the highest performing under a given set of conditions.

This review will focus on collating and comparing the experimental data of materials that have been reported to remove H_2S from oxygen-free gas mixtures with relatively high performance at room temperature in the last decade, in gas mixtures relevant for use in fuel cells. This includes metal oxides, activated carbon, mesoporous silicas, zeolites and MOFs. The aims of this review are to identify the highest performing materials in H_2S removal from gas streams at low temperatures, and to provide a comprehensive listing of these to facilitate further

research in this area. In order to compare the performance of the materials from different papers, experimental conditions such as feed gas composition, feed gas velocity, H_2S adsorption capacity and breakthrough concentration threshold are compared simultaneously. The units for above factors and H_2S adsorption capacities are:

- Feed gas composition: %,
- Feed gas velocity: cm/s,
- Breakthrough concentration threshold (BT concentration): ppmv,
- H_2S adsorption capacity: $mgH_2S/g_{adsorbent}$.

Where possible, experimental conditions and results from papers using different units from above have been converted into the same units. Not all papers reported regeneration of materials after H_2S exposure, therefore the regeneration performance of materials will only be summarised for high performing materials if available.

2. Metal Oxides

Many metal oxides have been studied for desulphurisation processes, especially at high temperatures. It is worth noting that the performance of the materials in adsorbing H_2S is influenced by many factors such as temperature, pressure, flow rate, feed compositions, breakthrough concentration definition, etc.[12]. Although zinc-based materials are recommended for high temperature (400 °C) desulphurisation [26], CuO was suggested to be more suitable for low temperature applications [27]. According to the sulfidation Gibbs free energy at 298 K (ΔG_{298}), the other promising transition-metal oxides for desulphurisation at room temperature include ZnO (−76 kJ/mol), NiO (−74 kJ/mol), CuO (−126 kJ/mol), Fe_2O_3 (−136 kJ/mol) and Co_3O_4 (−251 kJ/mol) [28, 29]. Figure 2 shows the adsorption capacities of metal oxides and their corresponding experimental condition parameters using data from references [27, 30-36]. There are two types of data being compared in Figure 2:

1) Static adsorption capacity: the adsorption capacity of the adsorbent when leaving the them in an equilibrium cell at a fixed temperature.
2) Dynamic adsorption capacity: the adsorption capacity of the adsorbent as the feed gas flows through them at a fixed flow rate, temperature and pressure [37].

The adsorption capacities of the first few metal oxides in Figure 2 are static adsorption capacities. Therefore, their feed gas velocity and breakthrough concentration threshold are not shown on the graph. As can be seen in Figure 2 (c), the CuO (283 $mgH_2S/g_{adsorbent}$) sample reported by Xue et al [27] shows the highest adsorption capacity compared to the other

materials. However, it is worth noting that their test result refers to static adsorption capacity, which provides the material with longer contact period and leads to higher adsorption capacity than dynamic adsorption processes [37].

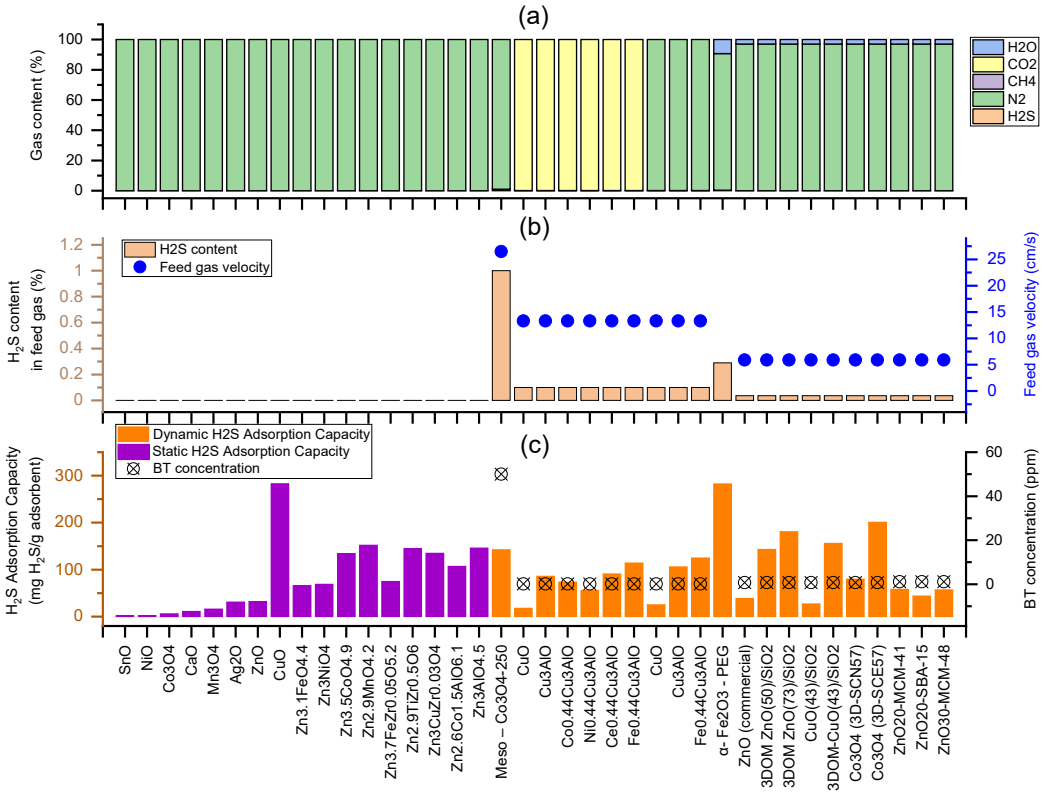

Figure 2. H_2S adsorption capacities of metal oxides and corresponding experimental condition parameters from reference [27, 30-36] (a) feed gas composition, (b) H_2S content in the feed gas and feed gas velocity, (c) breakthrough capacities of metal oxides and breakthrough concentration threshold

By comparing the dynamic adsorption capacity results in Figure 2 (c), the metal oxide that showed the highest H_2S adsorption capacity is α- Fe_2O_3 – PEG reported by Liu et al [30]. The authors prepared mesoporous iron oxides using solid-state reaction method with different structure-directing agents. The obtained samples were tested in gases consisting of 2900 ppmv H_2S, 9.3% H_2O, N_2 at ambient temperature at a space velocity of 7000 h^{-1}. The authors suggested that the structure directing agent (polyethylene glycol: PEG) increased the number of mesopores and surface hydroxyl groups in the metal oxide, which led to a higher performance. Despite showing the highest dynamic adsorption capacity (282.6 $mgH_2S/g_{adsorbent}$), the concentration of H_2S in the feed gas is also higher than many other papers (see Figure 2 (a) and (b)). In addition, there is a high level of water in the feed gas which will promote a higher adsorption capacity [38-42]. Due to the lack of sample bed dimension in the paper, the feed gas velocity cannot be identified and compared against other paper. Furthermore,

the breakthrough threshold concentration was not clarified in the paper, which could influence the adsorption capacity to a great extent.

The metal oxide based materials that showed the second and the third highest dynamic H_2S adsorption capacities in Figure 2 (c) are Co_3O_4 3D-SCE57 (201 $mgH_2S/g_{adsorbent}$) [35] and 3DOM $Zn(73)/SiO_2$ (181 $mgH_2S/g_{adsorbent}$) [32] reported by Wang et al, who have investigated synthesising metal oxides (ZnO, CuO, Co_3O_4, Fe_2O_3 etc.) and silica composites with three dimensionally ordered micropores (3DOM) structure [32, 34, 35, 40, 41]. The above materials were tested in feed gas consisting of 3% H_2O, 360 ppmv H_2S balanced by N_2. The authors suggested that silica contributed to the well-connected macropores, increased quantity of mesopores, and better dispersion of metal oxides. This resulted in the high performance of the materials. It is worth noting that this does not suggest Co_3O_4 and ZnO have higher adsorption capacity than the other metal oxide composites with similar structures. The amount of metal oxide in each composite is not the same. In addition, a quick comparison of the data in Figure 2 shows that their materials generally show much higher H_2S adsorption capacities than samples from other reports. This could be attributed to the effective structure in the materials introduced by their synthesis method. However, the authors also reported that moisture in the feed gas had a positive impact on the performance of the materials (performance improvement of 8.4 times). Similar phenomenon has also been reported by other researchers [38-42]. The moisture in the feed gas have been reported to enhance the adsorption capacity of the material by forming a water film on the surface of the material. The water film absorbs H_2S in the feed gas and disassociate the H_2S into HS^- and H^+. At the same time, the basic component of the adsorbents (e.g. ZnO) promotes alkalinisation of the water, making it easier to react with the dissolved H_2S [32, 43-46].

Considering the contribution of moisture and high H_2S content of comparable candidates [32], $Fe_{0.44}Cu_3AlO_x$ reported by Zhang et al would appear to exhibit a higher performance than other materials. The material was tested in N_2 with 1000 ppmv H_2S under a gas velocity of 13.3 cm/s. Despite the higher gas velocity (see Figure 2 (b)) and the lack of moisture, the material was able to show a high adsorption capacity (125 $mgH_2S/g_{adsorbent}$) [33]. However, the higher temperature which $Fe_{0.44}Cu_3AlO_x$ was tested under (40 °C in this paper vs 30 °C for Meso – Co_3O_4-250 in reference [31]) could help increase the adsorption capacity by assisting kinetics of the sulphur removal reaction and the diffusion of gases to the reaction sites [47].

3. Activated carbon

With its low price and high surface area, activated carbon is widely used in adsorption and catalytic processes. Activated carbon adsorption materials can be derived from various sources such as wood, coal, and others. Factors that influence H_2S adsorption performance include specific surface area, pore size, volume, surface chemistry, etc. In order to achieve high adsorption capacities for H_2S, activated carbon materials generally require modifications via either impregnation with chemicals or doping with heteroatoms [10, 11, 24, 48]. Activated carbon-based materials with relatively high H_2S adsorption capacities and corresponding experimental condition parameters using data from references [49-57] are summarised in Figure 3.

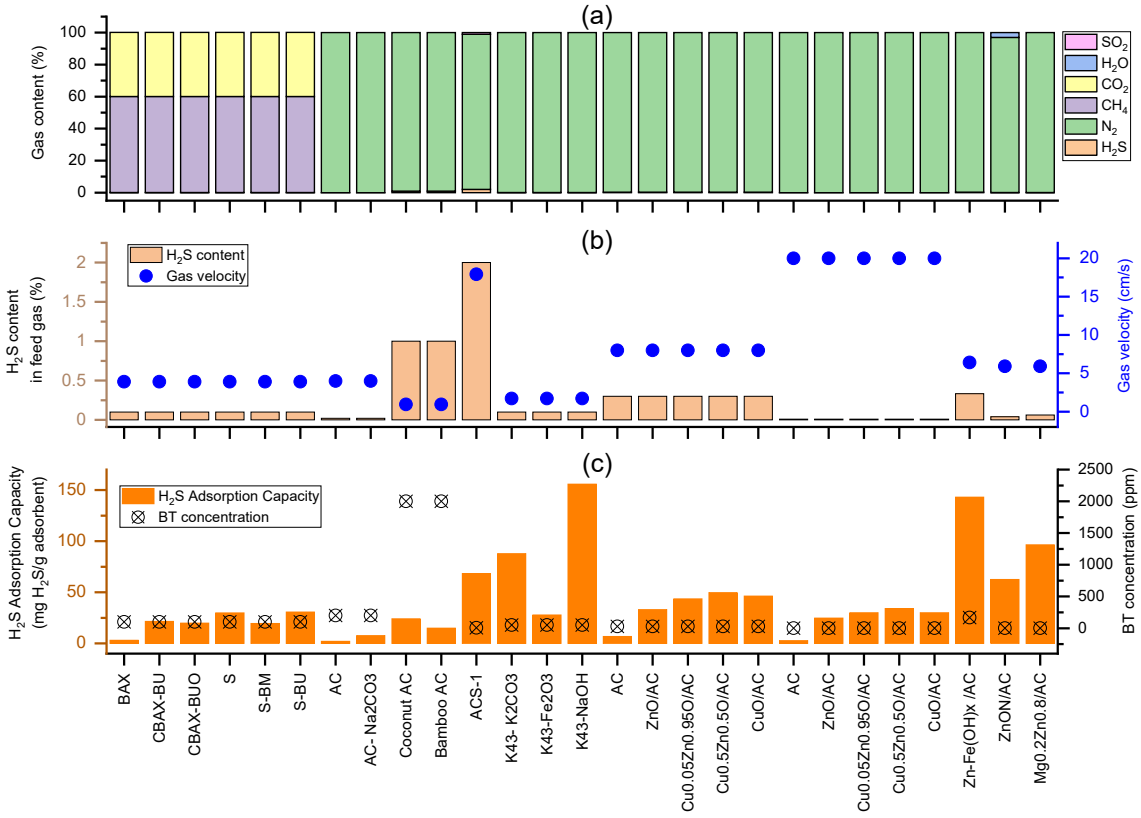

Figure 3. Breakthrough capacities of activated carbons and corresponding experimental condition parameters from reference [49-57] (a) feed gas composition, (b) H_2S content in the feed gas and feed gas velocity, (c) breakthrough capacities of activated carbons and breakthrough concentration threshold

From Figure 3 (c), the activated carbon material with the highest adsorption capacity is a commercial material Desorex K43-NaOH (155.72 $mgH_2S/g_{adsorbent}$) reported by Catrillon et al. The group carried out an H_2S adsorption test at 30 °C using a feed gas containing 1000 ppmv H_2S in N_2. The flow rate of the feed gas was 200 ml/min (velocity: 1.7 cm/s) [52]. The impregnated NaOH in Desorex K43-NaOH potentially formed NaHS and N_2S during the

breakthrough tests. The authors accredited the high H_2S adsorption capacity of the material to the surface basicity introduced by the impregnated NaOH. Despite the high adsorption capacity, it is worth noting that the breakthrough concentration threshold used in this paper was 50 ppmv, which is higher than some other reports (e.g. 6.59 ppmv for ACS-1 (activated carbon from coconut shell source) from Shi et al [51] and 0.11 ppmv for $Mg_{0.2}Zn_{0.8}$/AC from Yang et al [57]). Compared to using a lower breakthrough concentration threshold value, using a higher value means a later end time of the breakthrough test. With the extra time gained included in the calculation of adsorption capacities of the materials, a higher adsorption capacity value is obtained consequently. Besides, the gas velocity in their test is much lower than many other reports (see Figure 3 (b)), which meant a longer retention time, leading to a higher adsorption capacity [58-60].

The material showing the second highest H_2S adsorption capacity in Figure 3 (c) is Zn-Fe hydroxide/AC (10 wt%) (143 $mgH_2S/g_{adsorbent}$) reported by Lee et al. They used $ZnCl_2$, $FeCl_3$ and a different amount of peat-based activated carbon (0-30 wt%) to prepare bimetallic hydroxide materials under different conditions. The samples were tested in H_2S (3333 ppmv) in N_2 at a flow rate of 300 ml/min at room temperature. The Zn and Fe in Zn-Fe hydroxide/AC formed ZnS and FeS after breakthrough experiment. They were reported to have synergetic interactions, which improved the morphology and structure of the material, leading to an enhanced H_2S adsorption capacity [55]. It is worth noting that the concentration of H_2S in the feed gas is much higher than in many other papers (see Figure 3 (b)). The gas composition in this paper is closest to the report from Balsamo et al. [53] (3000 ppmv H_2S balanced by N_2). By comparison, the concentration of H_2S used for deciding breakthrough moments in this paper (166.7 ppmv) is much higher than other reports (e.g. 30 ppmv for $Cu_{0.5}Zn_{0.5}O$/AC from Balsamo et al. [53]). In addition, the gas velocity used in this paper (6.4 cm/s) is lower than that used by Balsamo et al. (velocity: 8 cm/s). These factors would also contribute to a higher adsorption capacity [58-60].

The material with the third highest H_2S adsorption capacity in Figure 3 (c) is $Mg_{0.2}Zn_{0.8}$/AC (96.5 $mgH_2S/g_{adsorbent}$) reported by Yang et al. The authors dispersed different molar ratios of MgO and ZnO (20 wt%. loading in total) onto coal based activated carbon pellets. The obtained materials were tested in N_2 containingH_2S (612.5 ppmv) gas at a flow rate of 100 ml/min (velocity: 5.9 cm/s) and 30 °C. The authors suggested that MgO enhanced the desulphurisation process by promoting the formation of HS^-, which could then react with ZnO or oxygen to

produce ZnS and S [57]. Despite the seemingly higher adsorption capacity value than their previous report [56], the concentration of the H_2S in the feed gas was also higher than the earlier report , which could also contribute to the higher adsorption capacity [56].

One material that is worth pointing out is a commercial activated carbon material of coconut-shell source (ACS-1: 69.3 mgH_2S/$g_{adsorbent}$) reported by Shi et al. The sample was tested in a feed gas containing 20, 000 ppmv H_2S, 10, 000 ppmv SO_2 in N_2 at 30 °C [51]. Despite a much higher sulphur content than other reports (see Figure 3 (a) and (b)) which would help with achieving a higher adsorption capacity, the SO_2 may also compete with H_2S by occupying micropores of the same size (0.5 nm) and reacting with adsorbed oxygen in the adsorbent [51]. This could lead to a lower H_2S adsorption capacity. Besides, the velocity of the feed gas was significantly higher than other reports (see Figure 3 (b)). Furthermore, the material can be regenerated completely and maintains stable performance for at least five continuous adsorption-regeneration cycles (see Figure 4) [51]. A high adsorption capacity at low retention times and positive stability characteristics during the regeneration process make the material a very promising candidate for sulphur removal.

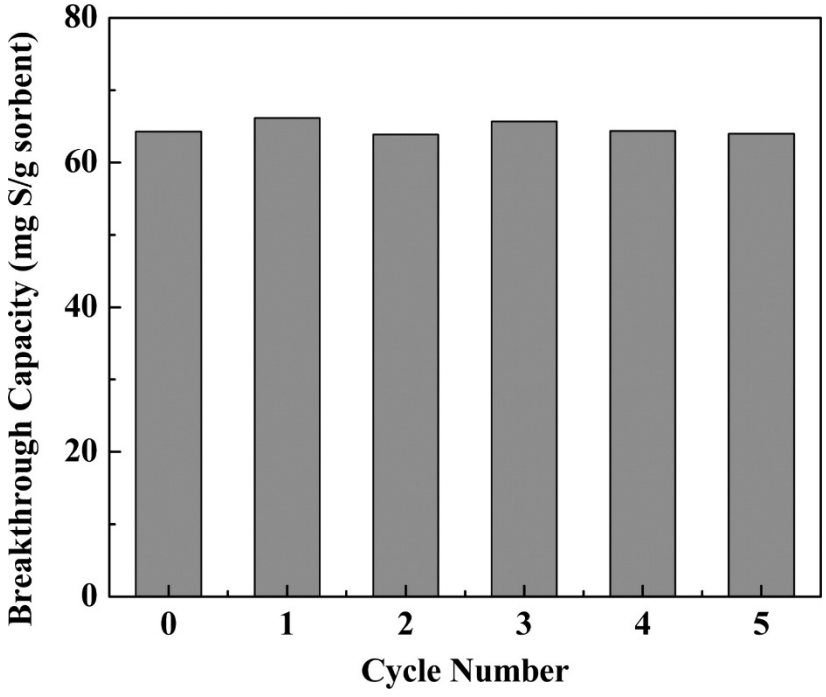

Figure 4. Breakthrough sulphur capacities of the ACS-1 sorbent over five adsorption–regeneration cycles (Reprinted with permission from [51]. Copyright (2019) American Chemical Society)

4. Zeolites

Zeolites are commonly used in a wide range of industries such as adsorbents for water purification and catalysts in the oil and gas industry. They are porous crystalline aluminosilicates with a general molecular formula of $M_{x/n}[(AlO_2)_x(SiO_2)_y] \cdot zH_2O$ (M are alkali or alkali earth elements). There are many types of zeolites with different structure and properties [11, 25, 48, 61, 62]. In general, the performance of unmodified zeolites in removing H_2S at low temperatures is poor [63-65]. Typically, the performance of zeolites can be improved by modifying the method of synthesis, exchanging the cations with other elements, and impregnating other chemicals (e.g. metal oxides) [65-72]. In this section, experimental data from various references, which report the performance of zeolites removing H_2S from various gases at temperatures between 25 °C and 40 °C, are summarised and compared in Figure 5 [63-72].

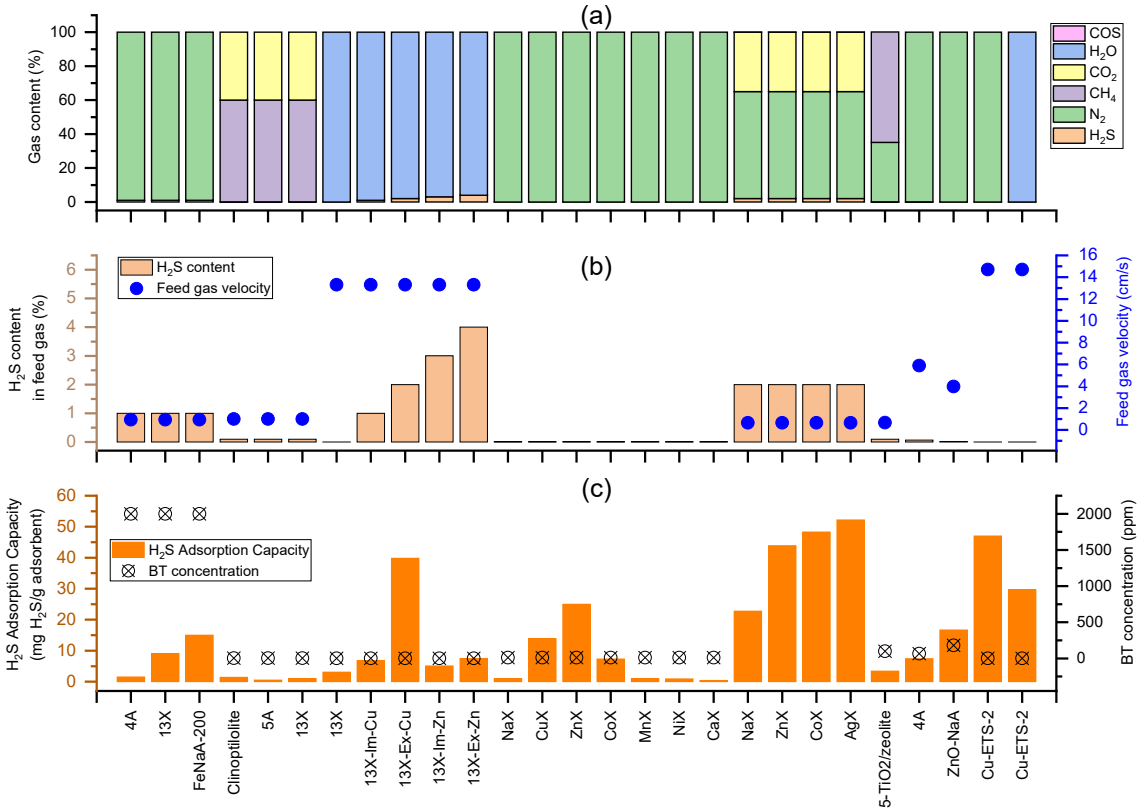

Figure 5. Breakthrough capacities of zeolites and corresponding experimental condition parameters from reference [63-72] (a) feed gas composition, (b) H_2S content in the feed gas and feed gas velocity, (c) breakthrough capacities of zeolites and breakthrough concentration threshold

The zeolite materials with the highest and the second highest adsorption capacity in Figure 5 (c) are AgX (Ag exchanged NaX: 52.7 $mgH_2S/g_{adsorbent}$) and CoX (Co exchanged NaX: 48.3

mgH_2S/$g_{adsorbent}$) reported by Chen et al [67]. The authors used an ion-exchange method and modified NaX with Zn, Co and Ag to remove sulphur from a feed gas (2% H_2S, 140 ppmv COS, 35% CO_2, 63% N_2) at a flow rate of 15 ml/min (velocity: 0.65 cm/s) at 25 °C. The AgX sample can also be regenerated with only 6.5% capacity loss. The regenerated sample was able to maintain its performance during the regeneration cycles in the paper (see Figure 6). The authors ascribed the enhanced sulphur adsorption capacities of sample to the chemisorption between H_2S and Ag^+ (sulphur-metal interaction) instead of physisorption [67]. Considering the potential competition from the high concentration of CO_2 in the feed gas, AgX seems to be a promising candidate for sulphur removal. However, the sulphur concentration in the feed gas is much higher than in other reports (e.g. 8 ppmv H_2S for 13X-Ex-Cu in ref [65]). Further, the velocity of the gas used is lower when compared to other papers (see Figure 5 (b)). Both these factors contribute to the demonstration of a higher adsorption capacity.

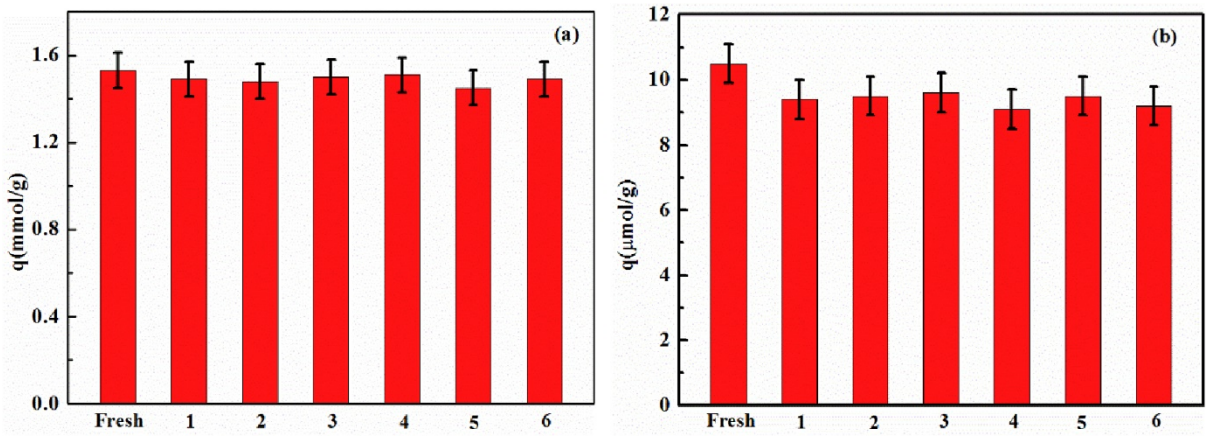

Figure 6. The breakthrough adsorption capacity for H_2S (a) and COS (b) adsorption on AgX regeneration (Reprinted from [67], with permission from Elsevier).

The zeolite material that shows third highest H_2S adsorption capacity in Figure 5 (c) is Cu exchanged Engelhard titanosilicate-2 (Cu-ETS-2: 12.5 wt% Cu) reported by Rezaei et al. The material was tested in N_2 containing10 ppmv H_2S at 25 °C using a gas flow rate of 100 ml/min (velocity: 14.7 cm/s). Three other commercial materials were also tested under the same conditions. The group showed that Cu-ETS-2 had a higher H_2S adsorption capacity (47 mgH_2S/$g_{adsorbent}$) than most commercial materials, apart from R3-11G (see Figure 7) [71]. However, despite a higher Cu content and a less competitive balancing gas (He instead of N_2) in the H_2S breakthrough test, the Cu-ETS-2 (13.2 wt% Cu) [72] reported by the same authors a few years later showed a lower H_2S adsorption capacity (29.7 mgH_2S/$g_{adsorbent}$) than the Cu-ETS-2 (12.5 wt% Cu (47 mgH_2S/$g_{adsorbent}$)) [71] in this paper. In reference [72], the authors used a similar method to exchange Engelhard titanosilicate-2 (Na-ETS-2) with different metal cations (Cu^{+2}, Ag^+, Zn^{2+}, Ca^{2+}). The samples and commercially available R3-11G were tested

in He with10 ppmv H_2S at 100 ml/min at room temperature [72]. Although Cu-ETS-2 (13.2 wt% Cu) showed a lower H_2S adsorption capacity than Cu-ETS-2 (12.5 wt% Cu), it showed a higher H_2S adsorption capacity than R3-11G (see Figure 8). By comparing the two tests, the higher adsorption capacity of Cu-ETS-2 (12.5 wt% Cu) in earlier test may be due to the discrepancy in surface structure and surface area caused by addition of Ludox HS-40 colloidal silica during granulation and smaller granule sizes (20-50 mesh [71] instead of 16-30 mesh [72]).

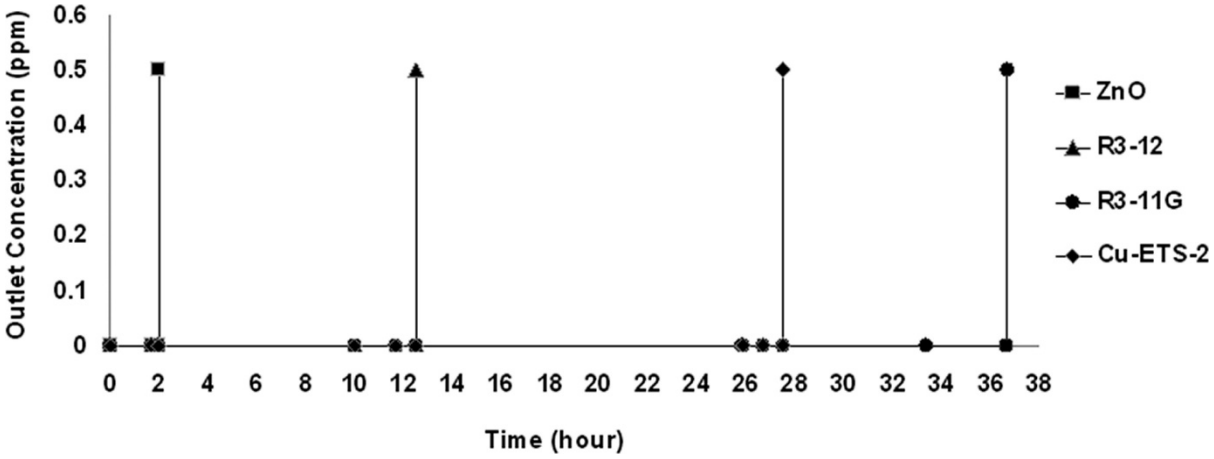

Figure 7. H_2S breakthrough times of Cu-ETS-2 (12.5 wt% Cu) and commercial adsorbents in N_2 with 10 ppmv H_2S (Reprinted from [71], Copyright (2012) American Chemical Society)

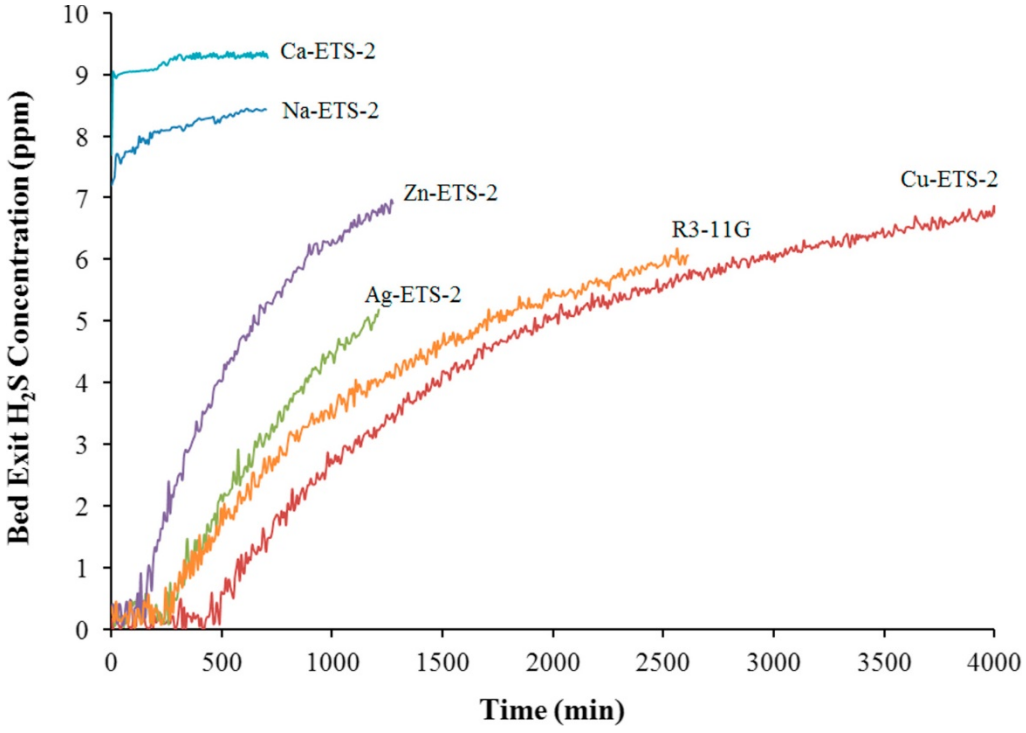

Figure 8. H_2S breakthrough times of R3-11G and Ag, Ca, Cu and Zn exchanged Na-ETS-2 in He with 10 ppmv H_2S (Reprinted from [72], with permission from Elsevier)

5. Mesoporous silica

With their large and uniform pore sizes, high surface area, and adjustable structures, mesoporous silica materials have attracted the attention of researchers in many fields such as catalysis, separation, and development of novel functional materials [73, 74]. Similar to zeolites, there are many types of mesoporous silica with different structures [73]. With their neutral frameworks, the H_2S adsorption capacity of silica materials cannot compete with other material classes. However, the structural properties of silica compounds make an excellent platform for other functional groups (e.g. amines, metal oxides, MOFs). Using data from references [36, 60, 75-89], the performance of silica materials and silica materials modified with different functional groups in removing H_2S from a range of gases is shown in Figure 9. According to Figure 9 (a) and (c), apart from the silica materials modified with ZIF-8 reported by Saeedirad et al [85] , materials tested in gases containing H_2O (highlighted in the red grid in Figure 9) generally show higher adsorption capacities than materials tested in dry gases. The presence of moisture in the gas has been reported to have a positive impact on the H_2S adsorption capacities of materials impregnated with metal oxides or amine [32, 90] . According to Wang et al, the performance of the material can be improved by up to 8.4 times when moisture exists in the gas [32]. With the potential of significant impact on the performance of the materials by moisture, it is challenging to compare materials tested with differing humidity of feed gas. Therefore, they will be compared separately.

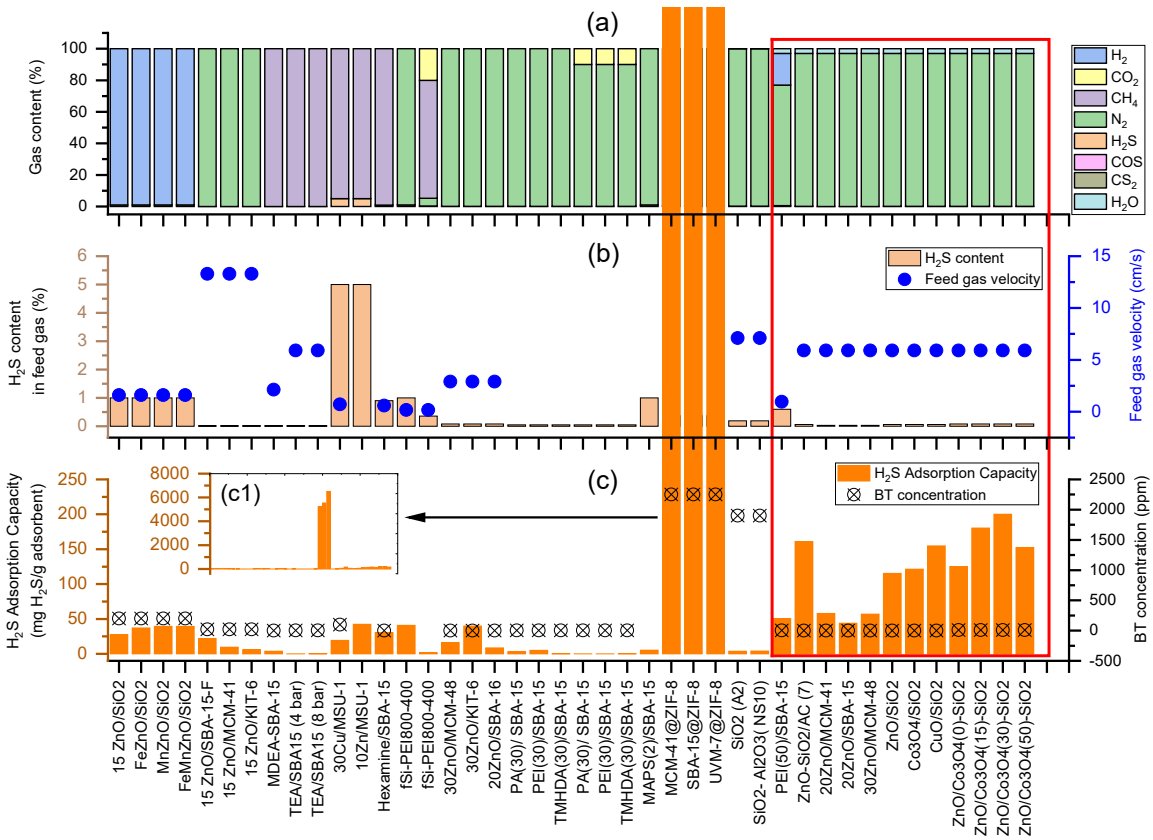

Figure 9. Breakthrough capacities of silica materials and corresponding experimental condition parameters from reference [36, 60, 75-89] (a) feed gas composition, (b) H_2S content in the feed gas and feed gas velocity, (c) breakthrough capacities of silica materials and breakthrough concentration threshold, (c1) zoomed out view of Figure 9 (c) showing breakthrough capacities of silica based materials that are significantly higher than the other silica based materials.

5.1 Silica based materials tested in dry gas

Among papers using dry feed gas in Figure 9, UVM-7@ZIF-8, MCM-41@ZIF-8, and SBA-15@ZIF-8 reported by Saeedirad et al show significantly higher adsorption capacities than the other materials (see Figure 9 (c1)). They used various silica materials (MCM-41, SBA-15 and UVM-7) as supports and grew ZIF-8 on them. Their H_2S adsorption tests were carried out in N_2(flow rate: 200 ml/min) containing 3699 ppmv H_2S at 30 °C. The adoption capacities of the samples (MCM-41, SBA-15 and UVM-7) were: 5228, 5536, and 6503 $mgH_2S/g_{adsorbent}$ respectively. Physical adsorption was reported to be the main process during H_2S removal. The authors suggested that the π-complexations formations between Zn active sites and 2-methylimidazole linkers in ZIF-8 contributed to the high performance of the materials. This was in addition to the mesopore structures and pore sizes of the silica materials. In addition, they can be regenerated with very little decrease in the adsorption capacities of samples even after three regeneration cycles (see Figure 10). With the highest adsorption capacity and

regeneration performance, UVM-7@ZIF-8 was suggested as a promising material for removing H_2S [85].

Compared to other silica-based materials, the adsorption capacities of these three materials are very high. However, it is worth noting that the concentration of H_2S in the feed gas in this paper was higher than many other reports (see Figure 9 (b)). In addition, the concentration of H_2S for defining breakthrough moment in this report (1849 ppmv) was much higher than other papers (see Figure 9 (c)), which will contribute to a higher adsorption capacity [86]. A closer examination of the breakthrough curve of UVM-7@ZIF-8 (see Figure 11) shows that using 1849 ppmv (50% of the H_2S concentration in feed gas) as the threshold value for breakthrough concentration correspond to approximately 400 min as the breakthrough time. However, if a lower H_2S concentration is used as the threshold value for breakthrough concentration (e.g. 5%), the corresponding breakthrough time would be about 320 min. Using the shorter time to calculate the breakthrough capacity of the sample would lead to at least 20% lower value than what was used by the authors. Aside from the results reported by Saeedirad et al [85], the H_2S adsorption capacity of silica-based samples from other reports are in the range of 5.8 $mgH_2S/g_{adsorbent}$ to 42.3 $mgH_2S/g_{adsorbent}$ when tested in dry gas.

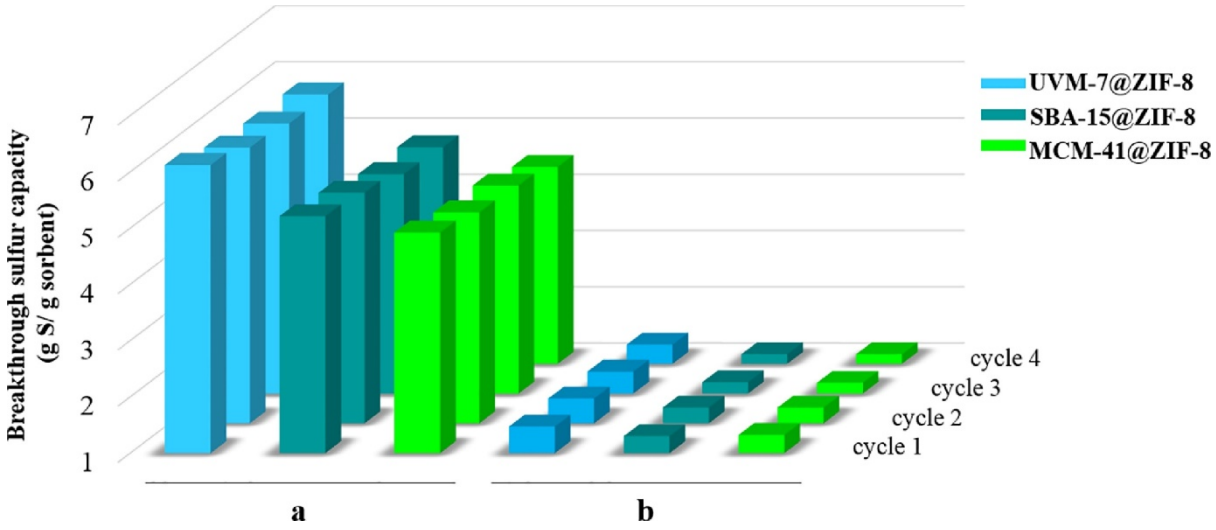

Figure 10. (a) H_2S and (b) CH_3CH_2SH adsorption capacities of hybrids after regeneration cycles (Reprinted from [85], with permission from Elsevier)

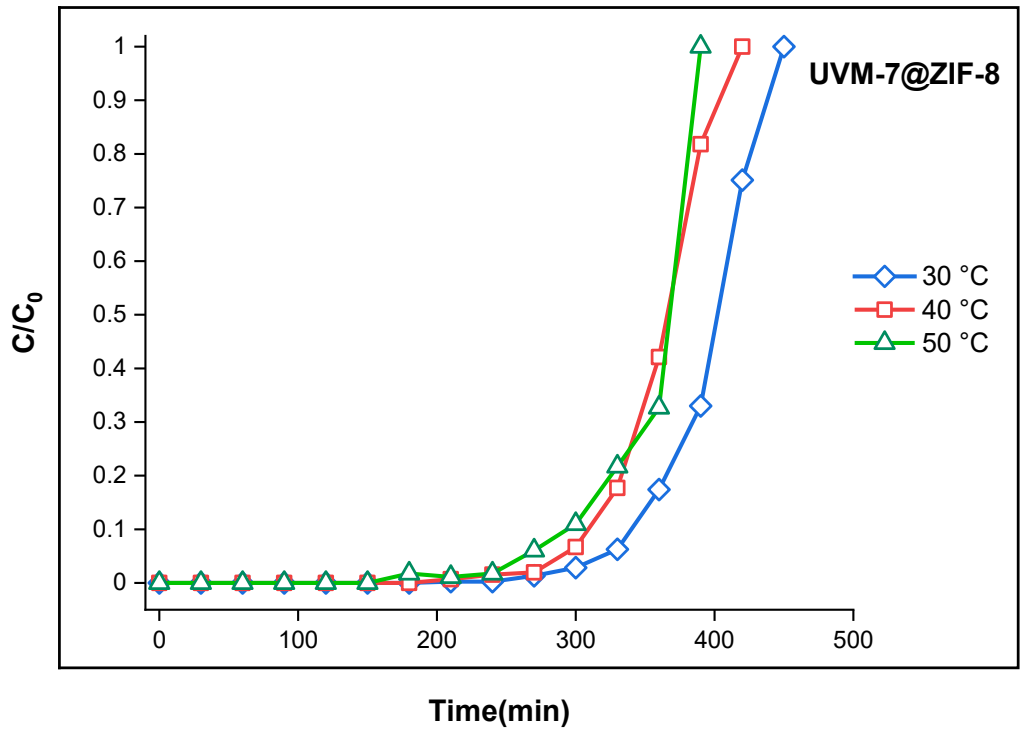

Figure 11. Breakthrough curves of UVM-7@ZIF-8 for removal of hydrogen sulfide at different temperatures (Reprinted from [85], with permission from Elsevier)

5.2 Silica based materials tested with wet gas

Compared to materials tested in dry gases, there are more materials showing H_2S adsorption capacities above 100 $mgH_2S/g_{adsorbent}$ (see Figure 9 (c)). In particular, ZnO/Co_3O_4 (30)-SiO_2 reported by Yang et al showed an adsorption capacity of 200.2 $mgH_2S/g_{adsorbent}$ and they prepared zinc-cobalt-silicon ternary material via a sol-gel method using different ratios of ZnO and Co_3O_4. The obtained samples were tested in gases containing 800 ppmv H_2S, 3% moisture with N_2 as balanced at 100 ml/min (velocity: 5.9 cm/s) at 30 °C [87]. Despite the high H_2S adsorption capacity, it is worth noting that the breakthrough concentration in their experiment (8 ppmv H_2S) was higher than other papers (e.g. 0.11 ppmv for CuO/SiO_2 in ref [88]). In another paper reported by the same authors, they used different amounts of AC and synthesised ZnO/SiO_2 using the sol-gel method [88]. Under the same gas flow rate and temperature as in reference [87], the sample that showed the highest adsorption capacity was $ZnO\text{-}SiO_2$/AC (7%) (161 $mgH_2S/g_{adsorbent}$) [88]. Although this is not as high as ZnO/Co_3O_4 (30)-SiO_2, the concentration of H_2S in the feed gas (622 ppmv [88] vs 800 ppmv [87]) and the breakthrough capacity concentration defined in this paper are much lower by comparison (0.11 ppmv instead of 8 ppmv as in ref [87]). The high adsorption capacity makes this material a promising

candidate for H_2S removal. However, it is worth noting that the H_2S adsorption capacity of the material decreased to 75 $mgH_2S/g_{adsorbent}$ (over 50% loss) after three regeneration cycles [88].

6. Metal Organic Frameworks

Metal organic frameworks (MOF) consist of metal ions or clusters linked by organic ligands. Both structure and properties may be tuned by combining different metal elements and organic linkers which makes them very attractive candidates for many applications [11, 22, 48, 91-95]. It is worth noting that the concentration of H_2S in feed gas compositions from different papers ranges from less than 100 ppmv to 15%, and some papers reporting pure H_2S isotherms of MOF materials. The adsorption capacities of MOFs obtained via their isotherms are very different from dynamic breakthrough capacities since the isotherm measurements are carried out with pure gas in a static environment. Because the concentration of the impurity gas and retention time could impact the performance of the materials [96-98], MOFs that measure pure H_2S isotherms are compared separately from the ones with dynamic adsorption capacities. For similar reasons, materials tested in feed gases with greater than 1% H_2S are compared separately.

6.1 H_2S adsorption capacities of MOF using pure H_2S

Figure 12 summarises H_2S adsorption capacity of MOFs using pure H_2S at 1 bar and 0.1 bar from references [99-112]. These data are from papers reporting H_2S adsorption isotherms at different temperatures and pressures. H_2S adsorption capacities at lower pressure are also listed here since the adsorption capacities of some MOFs can vary significantly with pressure. For example, the H_2S adsorption capacity of COF-6 decreased by 87.5% when the pressure of H_2S was reduced from 1 bar to 0.1 bar [109]. By contrast, there was only 24.3% decrease in H_2S adsorption capacity for MIL-47(V)-Br with the same pressure differential [110].

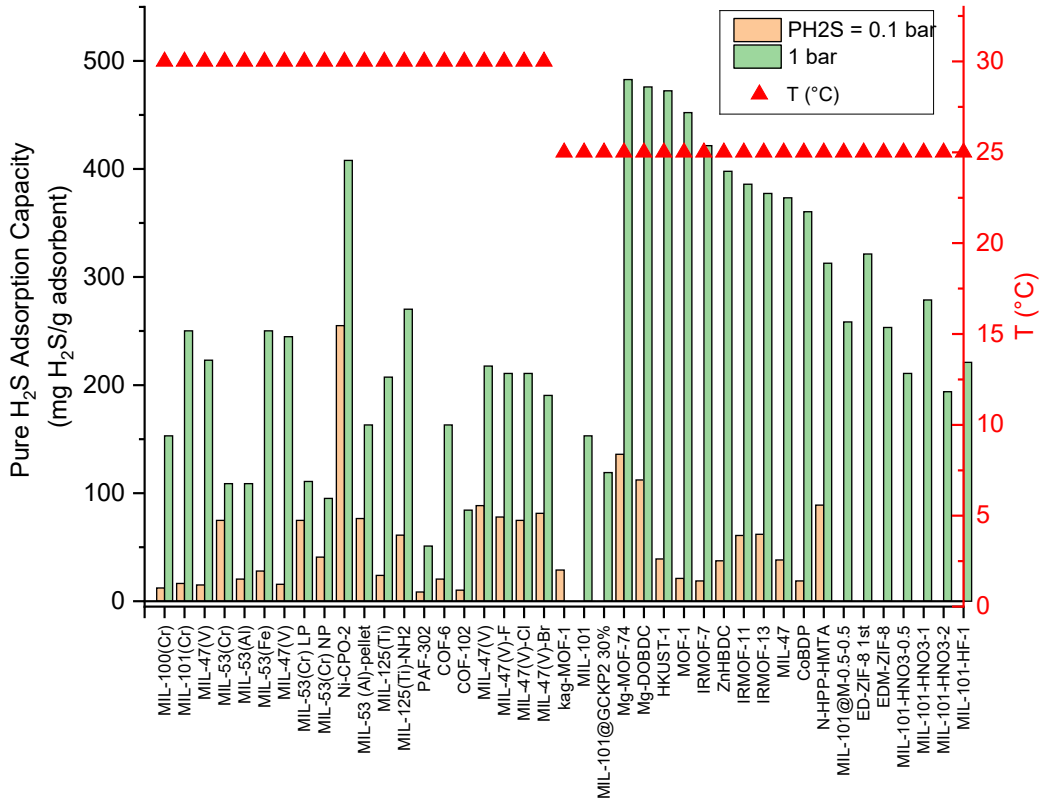

Figure 12. Adsorption capacities of MOF materials using pure H_2S at different partial pressures and temperatures from references [99-112]

From Figure 12, it seems that MOFs tested at 1 bar and 25 °C generally show much higher H_2S adsorption capacities than those tested at 1 bar 30 °C. However, the effect of temperature on the performance of MOFs varies with different materials. For example, MIL-47(V) [110] and IRMOF-3 [113] have been reported to show lower H_2S adsorption capacities as the working temperature increased. By contrast, HKUST-1 (MOF-199) has been reported to benefit from a higher working temperature [114, 115]. Furthermore, the simulation results from Zhang et al [116] showed a conflicting result from references [114, 115] and suggested that higher temperatures decreased the H_2S adsorption capacity of MOF-199. Due to the variance of performance of materials at different temperatures, the H_2S adsorption capacities of MOFs tested under the same temperature are compared and summarised below. By comparing H_2S adsorption capacities of different MOFs measured at 30 °C, MOF materials that show the three highest H_2S adsorption capacities at 1 bar are Ni-CPO-2 (408 $mgH_2S/g_{adsorbent}$) [100], MIL-125(Ti)-NH_2 (270.3 $mgH_2S/g_{adsorbent}$) [108], MIL-101(Cr) (250.2 $mgH_2S/g_{adsorbent}$) [102] and MIL-53(Fe) (250.2 $mgH_2S/g_{adsorbent}$) $mgH_2S/g_{adsorbent}$ [102]. At 25 °C and 1 bar, the top three MOF materials with high H_2S adsorption capacities are Mg-MOF-74 (482.8 $mgH_2S/g_{adsorbent}$), Mg-DOBDC (476 $mgH_2S/g_{adsorbent}$), and HKUST-1 (472.3 $mgH_2S/g_{adsorbent}$) reported by Zhou

et al [111]. The authors used molecular simulations to study the performance of 89 MOF materials in capturing toxic gases (NH_3, H_2S, NO_2, NO and CO). The report provides valuable information on the performance of MOF materials in capturing toxic gas. However, there is some difference between experimental and simulated results, despite the general agreement of simulated data trends with experimental results. Considering the discrepancies between experimental results and simulation, H_2S adsorption capacities of MOF materials obtained experimentally at 25 °C and 1 bar are also compared. Under these conditions, the top three performing MOF materials are ED-ZIF-8 1st (321.3 $mgH_2S/g_{adsorbent}$) [104], MIL-101-HNO_3-1 (278.8 $mgH_2S/g_{adsorbent}$) [107] and MIL-101@M-0.5-0.5 (258.4 $mgH_2S/g_{adsorbent}$) [99].

At 0.1 bar and 30 °C, MOF materials with the three highest experimentally obtained adsorption capacities are Ni-CPO-2 (255 $mgH_2S/g_{adsorbent}$) [100], MIL-53 (Al)-pellet (76.5 $mgH_2S/g_{adsorbent}$) [103], MIL-53(Cr) (74.8 $mgH_2S/g_{adsorbent}$) [102], and MIL-53(Cr)LP (74.8 $mgH_2S/g_{adsorbent}$) [102]. It is worth noting that Xu et al [110] used molecular simulations to evaluate the performance of MIL-47(V) and halogenated MIL-47(V) materials in adsorbing H_2S. The materials in the paper also displayed high H_2S adsorption capacities at 30 °C and 0.1 bar (74.8 - 86.2 $mgH_2S/g_{adsorbent}$). However, these values are much higher than the performance of the same material MIL-47(V) tested experimentally by Hamon et al (14.96 $mgH_2S/g_{adsorbent}$ [102] and 15.64 $mgH_2S/g_{adsorbent}$ [101]). With the vast difference between the simulation and experimentally obtained results, further research should be carried out to confirm the performance of the material at lower pressures. There are a limited number of papers reporting the H_2S adsorption capacities of MOF materials at lower pressures and 25 °C (see Figure 12). According to the molecular simulation of 89 MOF materials in adsorbing H_2S at 0.1 bar and 25 °C, the top three MOF materials are Mg-MOF-74 (136 $mgH_2S/g_{adsorbent}$), Mg-DOBDC (112.2 $mgH_2S/g_{adsorbent}$), and IRMOF-13 (61.9 $mgH_2S/g_{adsorbent}$) [111].

6.2 MOFs tested with low H_2S content in the feed gas

Figure 13 shows the H_2S breakthrough capacities of MOF materials tested in mixed gases containing various concentrations of H_2S so that the performance of MOFs under H_2S can be compared easily. The graph within the red grid in Figure 13 are for MOFs tested in gases containing 1% or less H_2S using data from references [103, 113-115, 117-121] and will be looked into more details in this section. The samples outside the red grid are for MOFs tested in gases containing more than 1% H_2S using the data from references [104, 122-126]. They will be discussed in more detail in the next section. According to the information in the red

grid in Figure 13 (c), the highest H_2S adsorption capacity is reported by Huang et al [118]. With the incorporation of glucose and graphene oxide (GO), they prepared Zn based MOF-5/GO composites with different amount of GO (1.75 - 7 wt%). The samples were tested in 100 ppmv H_2S in N_2 at 20 °C and 1 atm. At a gas flow rate of 300 ml/min (velocity = 17.7 cm/s) and breakthrough threshold of 1 ppmv H_2S, the sample that showed the highest H_2S adsorption capacity was MG-G3 (130.1 mgH_2S/$g_{adsorbent}$). The authors suggested that the high performance of the sample was due to the synergetic effect between glucose and GO when they are combined in the right ratio [118].

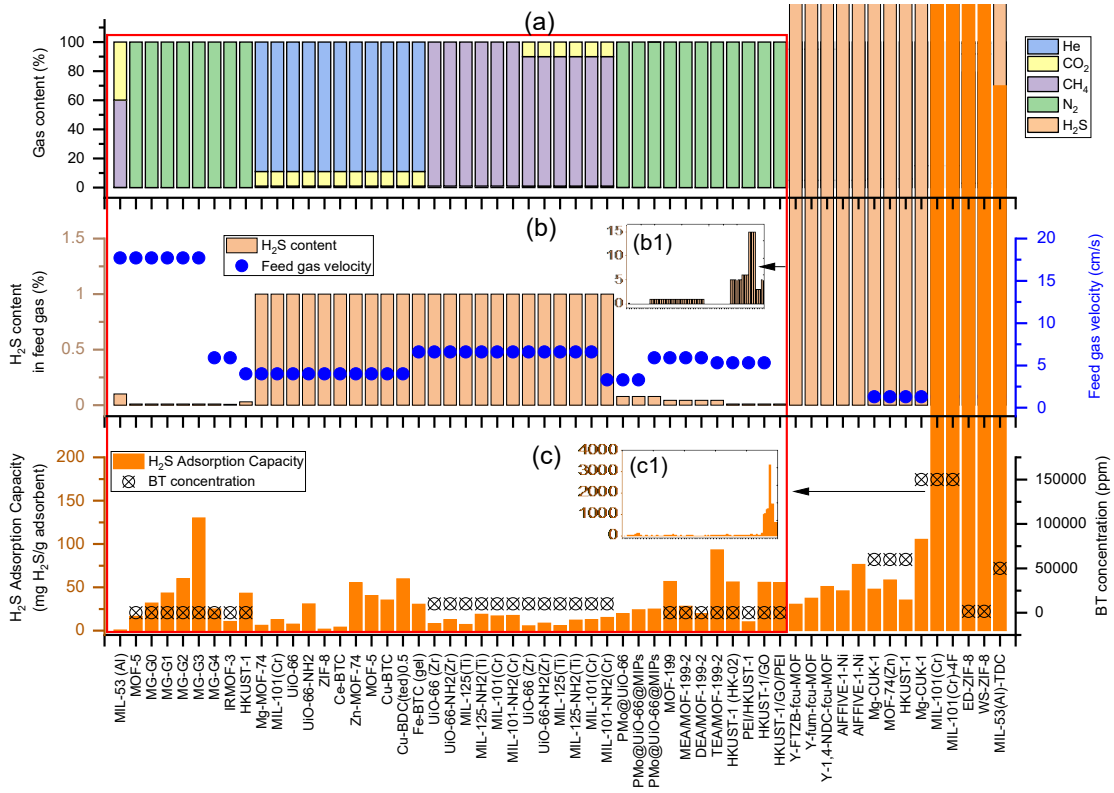

Figure 13. Breakthrough capacities of MOFs and corresponding experimental condition parameters from reference [103, 113-115, 117-126] (a) feed gas composition, (b) H_2S content in the feed gas and feed gas velocity, (b1) zoomed out view of Figure 13 (b) showing H_2S content in the feed gas that are significantly higher than other tests. (c) breakthrough capacities of MOFs and breakthrough concentration threshold, (c1) zoomed out view of Figure 13 (c) showing breakthrough capacities of MOFs that are significantly higher than other MOFs.

The MOF material with the second highest adsorption capacity was reported by Zhang et al. They impregnated different types of amine onto MOF-199 (also known as HKUST-1 or Cu-BTC). The feed gas for the desulphurisation test consisted of 438.7 ppmv H_2S in N_2. At 30 °C and a gas flow rate of 100 ml/min (velocity = 5.9 cm/s), the sample that showed the highest adsorption capacity was TEA/MOF-199-2 (93.2 mgH_2S/$g_{adsorbent}$) [121]. Although TEA/MOF-

199-2 [121] shows the second highest H_2S adsorption capacity among MOFs shown in the red grid in Figure 13 (c), it is worth noting that the concentration of the H_2S in the feed gas in this paper is also higher than some of the other papers (e.g. 99.6 ppmv H_2S in N_2 for HK-02 by Bhoria et al [115]). This would contribute to a higher adsorption capacity [125].

Bhoria et al used two types of copper nitrate hydrates to prepare HKUST-1 and modified them with two types of polyethyleneimine (PEI) and GO. The H_2S breakthrough tests at 25 °C used a feed gas (99.6 ppmv H_2S in N_2) flow rate of 40 ml/min (velocity = 5.3 cm/s). The samples synthesised using copper nitrate hemi pentahydrate generally showed higher H_2S adsorption capacities than the samples synthesised using copper nitrate hydrate. In addition, apart from PEI modified HKUST-1(P_HHK-02) showing a much lower H_2S adsorption capacity, the other HKUST-1 based samples of the copper nitrate hemi pentahydrate source showed similar H_2S adsorption capacities with the unmodified HKUST-1 (HK-02) showing the highest H_2S adsorption capacity (56.1 $mgH_2S/g_{adsorbent}$) [115]. Although the HK-02 based samples reported by Bhoria et al did not show as high H_2S adsorption capacity as TEA/MOF-199-2 [121], it is worth noting that the concentration of H_2S in the feed gas for HK-02 (99.6 ppmv H_2S in N_2) is only less than a quarter of that for TEA/MOF-199-2 (438.7 ppmv H_2S in N_2). Because higher feed concentrations have been reported to linearly increase the adsorption performance of material by assisting the gas diffusivity [60, 127]. This suggests that HK-02 may have a similar/better performance as TEA/MOF-199-2 in removing H_2S if they were tested under the same condition. This also indicates that the unmodified MOF-199 (feed gas: 438.7 ppmv H_2S in N_2) reported by Zhang et al [121] have lower/similar H_2S adsorption capacity to HK-02 (feed gas: 99.6 ppmv H_2S in N_2) [115] despite their similar H_2S adsorption capacity values.

The MOF material that showed the third highest adsorption capacity was reported by Liu et al. The authors tested the desulphurisation performance of 11 MOF materials in a feed gas consisting of 1% H_2S, 10% CO_2, and 89% He at 25 °C. The tests includes MOF-5, MOF-74 (Mg, Zn), ZIF-8, UiO-66, UiO-66(NH_2), MIL-101(Cr), M-BTC (Cu, Fe, Ce), and Cu-BDC(ted)$_{0.5}$. At a gas flow rate of 30 ml/min (velocity: 3.98 cm/s), the H_2S adsorption capacities of the samples are shown in Figure 14. By comparison, Cu-BDC(ted)$_{0.5}$ showed the highest H_2S adsorption capacity (59.8 $mgH_2S/g_{adsorbent}$) via chemisorption mechanism. However, the partial damage in its structure during the desulphurisation process also led to a much poorer performance after regeneration (see Figure 14). According to the breakthrough adsorption results, the tested MOF materials can be classified into two groups:

(1) One-off materials with high H_2S adsorption capacity and selectivity (Cu-BDC(ted)$_{0.5}$, Zn-MOF-74, MOF-5, Cu-BTC, UiO-66(NH_2)and MIL-100(Fe) gel). Most of the materials remove H_2S through chemical reactions between their metal centres and H_2S. Apart from UiO-66(NH_2) that could partially recover its performance, the structural impairment caused by the chemical reactions is not reversible for the other MOF materials.

(2) Reversible materials but with lower adsorption capacity and selectivity (MIL-101(Cr), UiO-66, Mg-MOF-74, Ce-BTC and ZIF-8). These materials remove H_2S through physical adsorption mechanisms and can be regenerated for repeated application. Materials in this group (UiO-66, Mg-MOF-74, and MIL-101(Cr)) were also recommended as candidate materials for H_2S removal by Liu et al. [120].

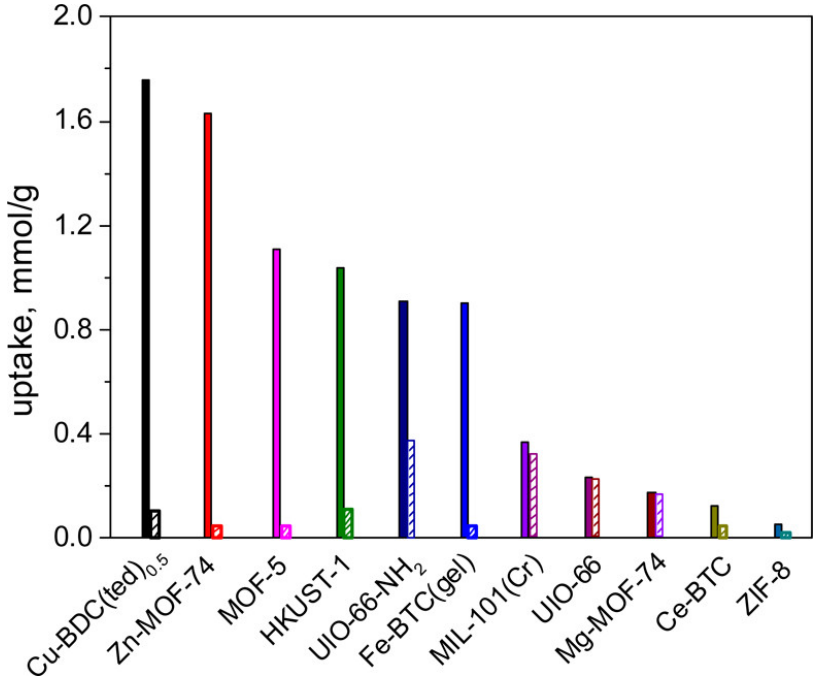

Figure 14. H_2S uptake on 11 MOF materials. The filled column refers to the uptake on fresh MOF adsorbents, and the striped column indicates that on the refreshed adsorbents (Adapted with permission from [120]. Copyright (2017) American Chemical Society)

6.3 MOFs tested with high H_2S content in the feed gas

For MOF materials that have been tested in feed gases with higher H_2S content (see Figure 15), the materials that showed the highest and the second highest desulphurisation performance are ED-ZIF-8 (3298 mgH_2S/g$_{adsorbent}$) and WS-ZIF-8 (1496 mgH_2S/g$_{adsorbent}$) as reported by Jamel et al [104]. They modified ZIF-8 nanoparticles with ethylenediamine (ED) using different methods and tested their desulphurisation performance in gases containing 3% H_2S, 7.3% CO_2, 1.0% He, 88.7% CH_4 at 25 °C at 2 bar. The authors suggested that the high surface area and

the increased H_2S affinity from amine additions led to the high H_2S adsorption capacities of the material. The adsorption process during sulphur removal involved both physical and chemical adsorption with physical adsorption being the main process. It was reported that the samples were able to maintain their structural stability after being regenerated under vacuum at 120 °C. It is worth noting that the more acidic CO_2 in the feed gas could compete with H_2S and lead to a lower H_2S adsorption capacity [11, 122]. According to Figure 15 (a), not all MOFs were tested in feed gases containing CO_2. Despite the presence of CO_2 in the feed gas, the fact that ED-ZIF-8 was able to show a higher adsorption capacity than other MOFs (see Figure 15 (c)) makes it a promising candidate material for H_2S removal. However, the flow rate and velocity of the feed gas were not specified in the paper. Besides, the pressure of the feed gas is higher than other papers, which would also contribute to the higher adsorption capacity [60, 127]. Furthermore, despite being structurally stable after regeneration, the desulphurisation performance of the regenerated samples was not reported. This is worth further investigation especially considering the absence of a peak ($2\theta = 32.3°$) in the XRD pattern of the sample after being regenerated [104].

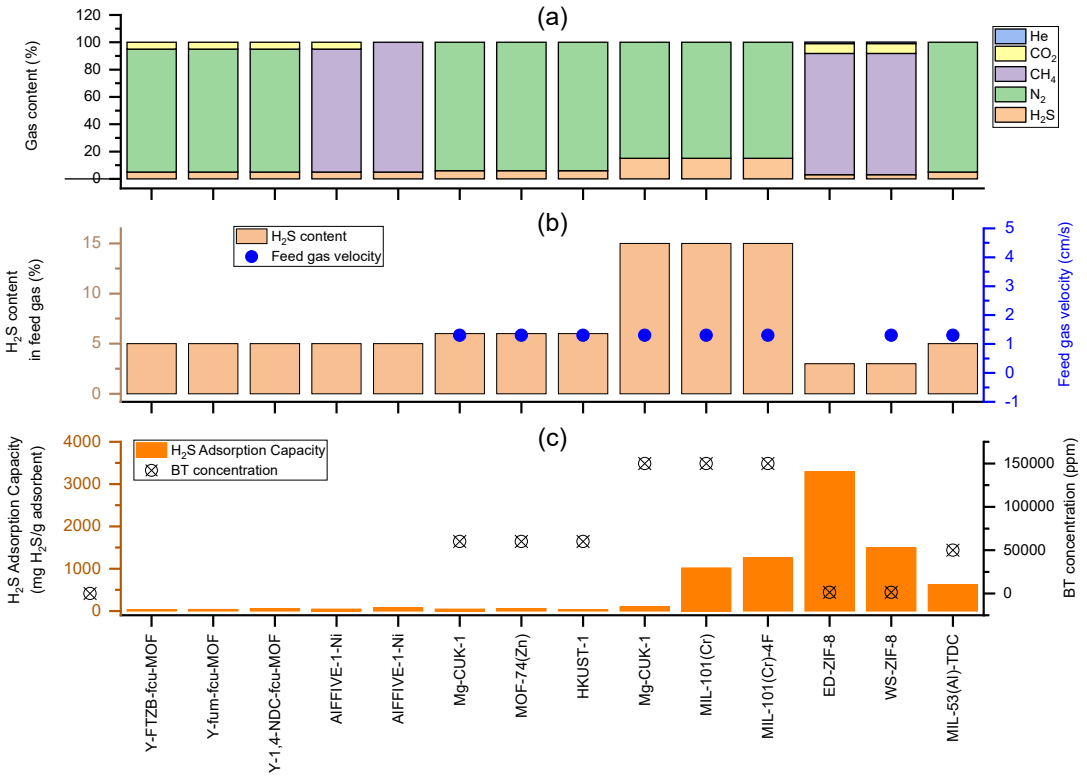

Figure 15. Breakthrough capacities of MOFs tested in high H_2S content in the feed gas and corresponding experimental condition parameters from reference [104, 122-126] (a) feed gas composition, (b) H_2S content in the feed gas and feed gas velocity, (c) breakthrough capacities of MOFs and breakthrough concentration threshold

Díaz-Ramírez et al prepared MIL-101(Cr)-4F(1%) by incorporating 2,3,5,6-tetrafluoro-1,4-benzenedicarboxylate (BDC-4F) into MIL-101(Cr) during the synthesis stage and tested the desulphurisation performance of the material at 30 °C and 0.689 bar [124]. Although the sample showed the third highest H_2S adsorption capacity in Figure 15, it is worth noting that the feed gas used in the desulphurisation test consisted of 15 vol% H_2S (balanced by N_2) which is significantly higher than the other papers (see Figure 15 (b)). In addition, the velocity of the feed gas (1.3 cm/s) is lower than many other papers (e.g. 17.7 cm/s for MG-G3 in ref [118]). The longer gas stream residence time would lead to a higher breakthrough capacity [58, 59]. Furthermore, the breakthrough capacity is calculated using the complete breakthrough time (saturation capacity). This also helped increase the H_2S adsorption capacity value by a large extent compared to using a lower breakthrough threshold (see Figure 16).

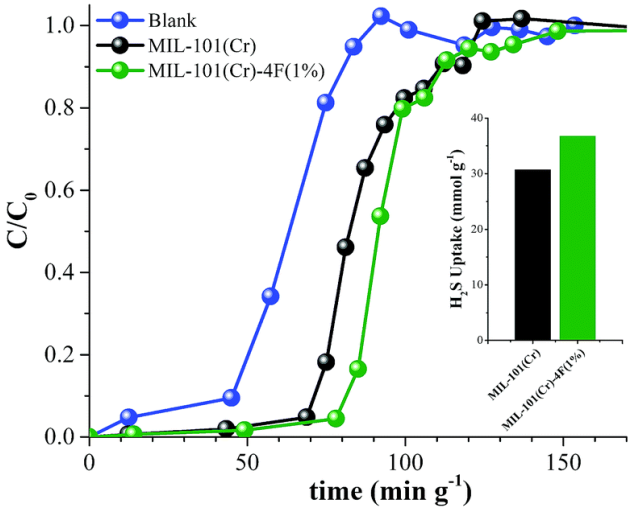

Figure 16. H_2S adsorption capacity of MIL-101(Cr) and MIL-101(Cr)-4F(1%) (Reproduced from Ref. [124] with permission from The Royal Society of Chemistry)

Another MOF material that showed relatively high H_2S adsorption capacity is MIL-53(Al)-TDC reported by Zárate et al. The authors tested the material in 5% H_2S and 95% N_2 at 30 ml/min (velocity: 1.3 cm/s) at 30 °C and 1 bar [126]. However, it is worth noting that, similar to the report from Díaz-Ramírez et al [124], the velocity of the feed gas in the desulphurisation test is relatively low and the breakthrough capacity is calculated using the complete breakthrough time (saturation capacity). Both of these factors would contribute to a higher breakthrough capacity value. Figure 17 (b) shows breakthrough curves of MOFs tested under similar conditions as MIL-53(Al)-TDC as shown in Figure 17 (a). By comparing the two figures, the H_2S almost breakthrough immediately at the beginning of the experiment for MIL-53(Al)-TDC (see Figure 17 (a)). By contrast, the increase in the concentration of H_2S in the exhaust gas happened much later in other materials (see Figure 17 (b)).

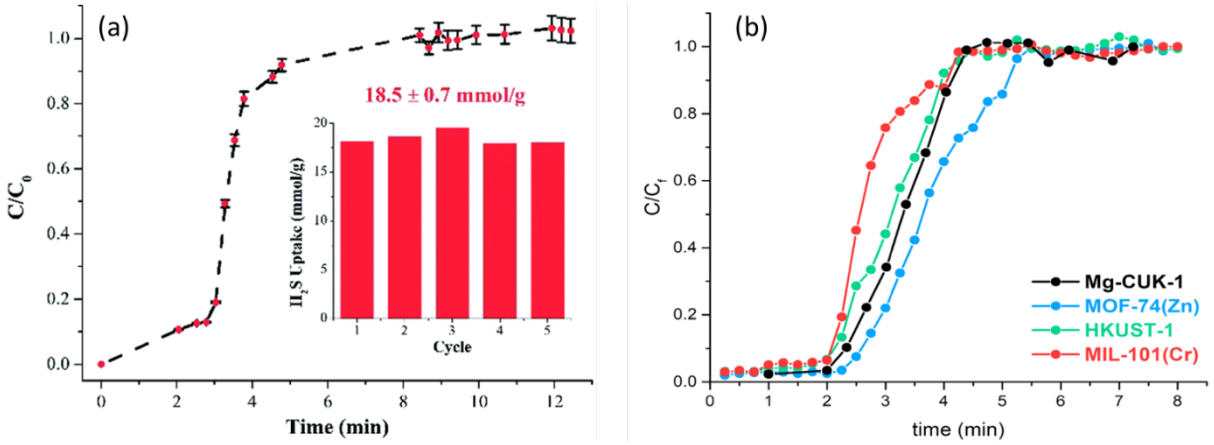

Figure 17. (a) Breakthrough curves of H_2S adsorption by MIL-53(Al)-TDC. The inset shows the comparative adsorption capacities for each cycle. (b) Breakthrough curves of H_2S adsorption by other MOFs (Reproduced from Ref. [126] with permission from The Royal Society of Chemistry)

7. Conclusion

With the benefits of lower energy consumption, using solid adsorbents to capture H_2S from oxygen-free gases at ambient temperature has attracted the attention of many researchers. The performance of common porous solid materials in removing H_2S from gas mixtures at low temperatures have been summarised in this review. With consideration of experimental conditions such as feed gas composition, gas velocity, and breakthrough concentration threshold, the performance is compared with high performing materials highlighted in each category. The material with the highest H_2S adsorption capacity (6503 $mgH_2S/g_{adsorbent}$) is UVM-7@ZIF-8 reported by Saeedirad et al [85]. This value is significantly higher than the adsorption capacity values of most other materials. The high adsorption capacity and its good stability make it a promising candidate material for H_2S removal. However, the cost of the material is much higher than traditional materials, such as activated carbon and zeolites which creates challenges for implementation commercially.

The second highest H_2S adsorption capacity was reported to be 3298 $mgH_2S/g_{adsorbent}$ shown by ED-ZIF-8 [94]. However, similar to UVM-7@ZIF-8, the cost of the material is again higher than the traditional adsorbent materials. Aside from the above two materials, the highest reported breakthrough capacities range from 40 to 283 $mgH_2S/g_{adsorbent}$ depending on the experimental conditions. The promising materials reported with high H_2S adsorption capacities in each material category are summarised below:

	Metal Oxide	**Activated carbons**	**Zeolites**	**Silica**	**MOF**
Highest	α- Fe_2O_3 – PEG [30]	Desorex K43-NaOH [52]	AgX [67]	UVM-7@ZIF-8 [85]	ED-ZIF-8 [104]
Breakthrough capacity (mg H_2S/g)	282.6	155.72	52.17	6503	3298
2nd Highest	Co_3O_4 (3D-SCE57) [35]	Zn-$Fe(OH)_X$ /AC [55]	CoX [67]	SBA-15@ZIF-8 [85]	WS-ZIF-8 [104]
Breakthrough capacity (mg H_2S/g)	201	143	48.28	5536	1496
3rd Highest	3DOM Zn(73)/SiO_2 [32]	$Mg_{0.2}Zn_{0.8}$/AC [57]	ZnX [67]	MCM-41@ZIF-8 [85]	MG-G3 [118]
Breakthrough capacity (mg H_2S/g)	181	96.5	43.86	5228	130.1
4th Highest	$Fe_{0.44}Cu_3AlO_x$ [33]	ACS-1 [51]	Cu-ETS-2 [71]	ZnO/Co_3O_4(30) -SiO_2 [87]	HK-02 [115]
Breakthrough capacity (mg H_2S/g)	114	68.3	47	200.2	56.1

It is worth noting that the order of the materials summarised in the table does not represent the absolute performance of the materials since many of them were tested under different conditions. The table aims to provide an overview of high performing materials that have been reported in each material category. Readers should look into the detailed test conditions of the materials.

Although some MOFs and silica-based materials showed significantly higher H_2S adsorption capacities than the other groups of materials, they are relatively novel materials by comparison and are not as commercially available on a mass scale. The stability of MOFs during operation is another aspect that should be improved for practical applications. In addition, the cost of producing MOFs and silica-based materials are much higher by comparison. Therefore, metal oxides, activated carbons and zeolites seem to be better candidates for practical applications in room temperature sulphur removal. In addition to identifying high performing materials, the following issues were identified and present opportunities for further research:

1. The main fuel gases for fuel cells are CH_4 or H_2. However, most papers use N_2 as the main balance gas. There exists a limited number of papers using CH_4 as the balance gas, with a correspondingly low number of papers presenting H_2 as balance gas. As the results listed in this paper show, a given material can have different selectivities for different gases, the balance gas can greatly influence the adsorption performance of a material. This is a particularly important effect to consider when using CH_4 as the feed gas or where high concentrations of impurities may exist such as CO_2 which is known to competitively adsorb onto the surface of the materials. Future research should place more focus on understanding the H_2S selectivities over other gases for different materials, and testing materials in feed gases that have closer compositions to industrial gases.
2. A majority of prior papers use feed gas compositions containing between 100 ppmv and 15 vol% H_2S. There is a very limited number of papers reporting the performance of materials removing H_2S from gases containing very low concentrations (e.g. 10 - 20 ppmv). With the wide range of H_2S content in industrial gases and the influence of H_2S concentration on the performance of the adsorbents, more research should be carried out on effective adsorbents for removing H_2S from gases with low H_2S concentrations. This is not only important for fuel cell applications, but also in the range of impurities typically found in biogases [128-130].
3. There currently exists uncertainty in the concentration of H_2S used to identify the breakthrough point of given materials in several papers included in this review. The selection of the breakthrough point concentration has a significant influence on the reported adsorption capacity of a material leading in some cases to much higher capacities than typically expected for a given material class. Therefore, future research should clearly define the H_2S concentration used for breakthrough point identification.
4. Temperature, flow rate (velocity) and gas composition among others, influence the performance of materials in removing H_2S from process gas streams. Further research into the effect of each operating condition may assist in performing comparative analyses of different adsorbents with different experimental conditions. However, many researchers used the traditional method of testing one variable at a time to investigate the impact of each factor. This makes it difficult to quantify the impact of each factor and have a comparative analysis of different adsorbents with different experimental conditions. A potential solution to the issue is using the Design of Experiments approach for future experiment designs, and build mathematical models

to better understand the impact of various experimental factors on the performance of adsorbents.

5. Materials such as impregnated activated carbons and MOFs have been reported to show poor performance after regeneration. Many of the papers examined in this review have omitted any reference to material regeneration. In identifying materials for hydrogen sulfide removal, it is important to consider material regeneration, which will play a significant role in practical applications. Therefore, more attention should be paid to investigating regenerating materials and to make sure they are stable in the long term in future research.

Acknowledgements

The authors gratefully acknowledge funding under grant KTP 11326 from Innovate UK, the Knowledge Transfer Partnerships and NanoSUN Ltd.

8. References

[1] FUEL CELLS and HYDROGEN 2 JOINT UNDERTAKING (FCH 2 JU) 2019 ANNUAL WORK PLAN and BUDGET. 2018.
[2] Kirubakaran A, Jain S, Nema RK. A review on fuel cell technologies and power electronic interface. Renewable and Sustainable Energy Reviews. 2009;13:2430-40.
[3] Kohl AL, Nielsen R. Gas purification: Elsevier; 1997.
[4] Höök M, Aleklett K. Historical trends in American coal production and a possible future outlook. International Journal of Coal Geology. 2009;78:201-16.
[5] Besancon BM, Hasanov V, Imbault-Lastapis R, Benesch R, Barrio M, Mølnvik MJ. Hydrogen quality from decarbonized fossil fuels to fuel cells. International Journal of Hydrogen Energy. 2009;34:2350-60.
[6] Treese SA. Hydrogen Production and Management for Petroleum Processing. In: Treese SA, Jones DS, Pujado PR, editors. Handbook of Petroleum Processing. Cham: Springer International Publishing; 2015. p. 1-67.
[7] Cui H, Turn SQ, Keffer V, Evans D, Tran T, Foley M. Contaminant Estimates and Removal in Product Gas from Biomass Steam Gasification. Energy & Fuels. 2010;24:1222-33.
[8] Fail S, Diaz N, Benedikt F, Kraussler M, Hinteregger J, Bosch K, et al. Wood Gas Processing To Generate Pure Hydrogen Suitable for PEM Fuel Cells. ACS Sustain Chem Eng. 2014;2:2690-8.
[9] Yin H, Yip ACK. A review on the production and purification of biomass-derived hydrogen using emerging membrane technologies. Catalysts. 2017;7.
[10] Abdoulmoumine N, Adhikari S, Kulkarni A, Chattanathan S. A review on biomass gasification syngas cleanup. Applied Energy. 2015;155:294-307.
[11] Shah MS, Tsapatsis M, Siepmann JI. Hydrogen Sulfide Capture: From Absorption in Polar Liquids to Oxide, Zeolite, and Metal–Organic Framework Adsorbents and Membranes. Chemical Reviews. 2017;117:9755-803.
[12] Cheng X, Shi Z, Glass N, Zhang L, Zhang J, Song D, et al. A review of PEM hydrogen fuel cell contamination: Impacts, mechanisms, and mitigation. Journal of Power Sources. 2007;165:739-56.
[13] Shabani B, Hafttananian M, Khamani S, Ramiar A, Ranjbar AA. Poisoning of proton exchange membrane fuel cells by contaminants and impurities: Review of mechanisms, effects, and mitigation strategies. Journal of Power Sources. 2019;427:21-48.
[14] Discepoli G, Desideri U, Cinti G, Massa R, Cruciani D. Analysis of performance decay of MCFC single cell under H2S poisoning. EFC 2009 - Piero Lunghi Conference, Proceedings of the 3rd European Fuel Cell Technology and Applications Conference2009. p. 341-2.
[15] Cigolotti V, McPhail S, Moreno A, Yoon SP, Han JH, Nam SW, et al. MCFC fed with biogas: Experimental investigation of sulphur poisoning using impedance spectroscopy. International Journal of Hydrogen Energy. 2011;36:10311-8.
[16] Monteleone G, De Francesco M, Galli S, Marchetti M, Naticchioni V. Deep H2S removal from biogas for molten carbonate fuel cell (MCFC) systems. Chemical Engineering Journal. 2011;173:407-14.
[17] Energy USDo, Ohi JM, Vanderborgh N, Voecks G. Hydrogen Fuel Quality Specifications for Polymer Electrolyte Fuel Cells in Road Vehicles. 2016.
[18] Nour Shafik El-Gendy JGS. Handbook of Refinery Desulfurization. Boca Raton CRC Press 2015.
[19] Stewart M, Arnold K. Part 1 - Gas Sweetening1,2
Gas Sweetening and Processing Field Manual. Boston: Gulf Professional Publishing; 2011. p. 1-140.

[20] Ahmad W, Sethupathi S, Kanadasan G, Lau LC, Kanthasamy R. A review on the removal of hydrogen sulfide from biogas by adsorption using sorbents derived from waste. 2019:20180048.
[21] Georgiadis A, Charisiou N, Goula M. Removal of Hydrogen Sulfide From Various Industrial Gases: A Review of The Most Promising Adsorbing Materials. Catalysts. 2020;10:521.
[22] Peluso A, Gargiulo N, Aprea P, Pepe F, Caputo D. Nanoporous Materials as H2S Adsorbents for Biogas Purification: a Review. Separation & Purification Reviews. 2019;48:78-89.
[23] Saji VS. Research advancements in sulfide scavengers for oil and gas sectors. 2019:20190049.
[24] Kailasa SK, Koduru JR, Vikrant K, Tsang YF, Singhal RK, Hussain CM, et al. Recent progress on solution and materials chemistry for the removal of hydrogen sulfide from various gas plants. Journal of Molecular Liquids. 2020;297:111886.
[25] Liu D, Li B, Wu J, Liu Y. Sorbents for hydrogen sulfide capture from biogas at low temperature: a review. Environmental Chemistry Letters. 2020;18:113-28.
[26] Elseviers WF, Verelst H. Transition metal oxides for hot gas desulphurisation. Fuel. 1999;78:601-12.
[27] Xue M, Chitrakar R, Sakane K, Ooi K. Screening of adsorbents for removal of H2S at room temperature. Green Chemistry. 2003;5:529-34.
[28] Baird T, Denny PJ, Hoyle R, McMonagle F, Stirling D, Tweedy J. Modified zinc oxide absorbents for low-temperature gas desulfurisation. Journal of the Chemical Society, Faraday Transactions. 1992;88:3375-82.
[29] Jiang D, Su L, Ma L, Yao N, Xu X, Tang H, et al. Cu–Zn–Al mixed metal oxides derived from hydroxycarbonate precursors for H2S removal at low temperature. Applied Surface Science. 2010;256:3216-23.
[30] Liu X, Meng X, Zhao J. Synthesis of nanocrystalline iron oxides with mesostructure as desulfurizer. Materials Letters. 2013;92:255-8.
[31] Pahalagedara LR, Poyraz AS, Song W, Kuo C-H, Pahalagedara MN, Meng Y-T, et al. Low Temperature Desulfurization of H2S: High Sorption Capacities by Mesoporous Cobalt Oxide via Increased H2S Diffusion. Chemistry of Materials. 2014;26:6613-21.
[32] Wang L-J, Fan H-L, Shangguan J, Croiset E, Chen Z, Wang H, et al. Design of a Sorbent to Enhance Reactive Adsorption of Hydrogen Sulfide. ACS Applied Materials & Interfaces. 2014;6:21167-77.
[33] Liu D, Chen S, Fei X, Huang C, Zhang Y. Regenerable CuO-Based Adsorbents for Low Temperature Desulfurization Application. Industrial & Engineering Chemistry Research. 2015;54:3556-62.
[34] Wang J, Wang L, Fan H, Wang H, Hu Y, Wang Z. Highly porous copper oxide sorbent for H2S capture at ambient temperature. Fuel. 2017;209:329-38.
[35] Wang J, Yang C, Zhao Y-R, Fan H-L, Wang Z-D, Shangguan J, et al. Synthesis of Porous Cobalt Oxide and Its Performance for H2S Removal at Room Temperature. Industrial & Engineering Chemistry Research. 2017;56:12621-9.
[36] Geng Q, Wang L-J, Yang C, Zhang H-Y, Zhao Y-R, Fan H-L, et al. Room-temperature hydrogen sulfide removal with zinc oxide nanoparticle/molecular sieve prepared by melt infiltration. Fuel Processing Technology. 2019;185:26-37.
[37] Mokhatab S, Poe WA, Mak JY. Chapter 9 - Natural Gas Dehydration and Mercaptans Removal. In: Mokhatab S, Poe WA, Mak JY, editors. Handbook of Natural Gas Transmission and Processing (Fourth Edition): Gulf Professional Publishing; 2019. p. 307-48.

[38] Davidson JM, Denny PJ, Lawrie CH. Autocatalysis by water in the reaction of hydrogen sulphide with zinc oxide. Journal of the Chemical Society, Chemical Communications. 1989:1695-6.
[39] Davidson JM, Lawrie CH, Sohail K. Kinetics of the absorption of hydrogen sulfide by high purity and doped high surface area zinc oxide. Industrial & Engineering Chemistry Research. 1995;34:2981-9.
[40] Fan H-L, Sun T, Zhao Y-P, Shangguan J, Lin J-Y. Three-Dimensionally Ordered Macroporous Iron Oxide for Removal of H2S at Medium Temperatures. Environmental Science & Technology. 2013;47:4859-65.
[41] Huang G, He E, Wang Z, Fan H, Shangguan J, Croiset E, et al. Synthesis and Characterization of γ-Fe2O3 for H2S Removal at Low Temperature. Industrial & Engineering Chemistry Research. 2015;54:8469-78.
[42] Zhao Y, Zhang Z, Yang C, Fan H, Wang J, Tian Z, et al. Critical Role of Water on the Surface of ZnO in H2S Removal at Room Temperature. Industrial & Engineering Chemistry Research. 2018;57:15366-74.
[43] Sitthikhankaew R, Chadwick D, Assabumrungrat S, Laosiripojana N. Effects of humidity, O2, and CO2 on H2S adsorption onto upgraded and KOH impregnated activated carbons. Fuel Processing Technology. 2014;124:249-57.
[44] Raymand D, van Duin ACT, Goddard WA, Hermansson K, Spångberg D. Hydroxylation Structure and Proton Transfer Reactivity at the Zinc Oxide−Water Interface. The Journal of Physical Chemistry C. 2011;115:8573-9.
[45] Huang C-C, Chen C-H, Chu S-M. Effect of moisture on H2S adsorption by copper impregnated activated carbon. Journal of Hazardous Materials. 2006;136:866-73.
[46] He R, Xia F-F, Wang J, Pan C-L, Fang C-R. Characterization of adsorption removal of hydrogen sulfide by waste biocover soil, an alternative landfill cover. Journal of Hazardous Materials. 2011;186:773-8.
[47] Sadegh-Vaziri R, Babler MU. Removal of Hydrogen Sulfide with Metal Oxides in Packed Bed Reactors—A Review from a Modeling Perspective with Practical Implications. Applied Sciences. 2019;9:5316.
[48] Khabazipour M, Anbia M. Removal of Hydrogen Sulfide from Gas Streams Using Porous Materials: A Review. Industrial & Engineering Chemistry Research. 2019;58:22133-64.
[49] Seredych M, Bandosz TJ. Desulfurization of Digester Gas on Wood-Based Activated Carbons Modified with Nitrogen: Importance of Surface Chemistry. Energy & Fuels. 2008;22:850-9.
[50] Seredych M, Bandosz TJ. Role of Microporosity and Nitrogen Functionality on the Surface of Activated Carbon in the Process of Desulfurization of Digester Gas. The Journal of Physical Chemistry C. 2008;112:4704-11.
[51] Shi L, Yang K, Zhao Q, Wang H, Cui Q. Characterization and Mechanisms of H2S and SO2 Adsorption by Activated Carbon. Energy & Fuels. 2015;29:6678-85.
[52] Castrillon MC, Moura KO, Alves CA, Bastos-Neto M, Azevedo DCS, Hofmann J, et al. CO2 and H2S Removal from CH4-Rich Streams by Adsorption on Activated Carbons Modified with K2CO3, NaOH, or Fe2O3. Energy & Fuels. 2016;30:9596-604.
[53] Balsamo M, Cimino S, de Falco G, Erto A, Lisi L. ZnO-CuO supported on activated carbon for H2S removal at room temperature. Chemical Engineering Journal. 2016;304:399-407.
[54] Falco Gd, Montagnaro F, Balsamo M, Erto A, Deorsola FA, Lisi L, et al. Synergic effect of Zn and Cu oxides dispersed on activated carbon during reactive adsorption of H2S at room temperature. Microporous and Mesoporous Materials. 2018;257:135-46.
[55] Lee S, Kim D. Enhanced adsorptive removal of hydrogen sulfide from gas stream with zinc-iron hydroxide at room temperature. Chemical Engineering Journal. 2019;363:43-8.

[56] Yang C, Yang S, Fan H, Wang Y, Shangguan J. Tuning the ZnO-activated carbon interaction through nitrogen modification for enhancing the H2S removal capacity. J Colloid Interface Sci. 2019;555:548-57.
[57] Yang C, Wang Y, Fan H, de Falco G, Yang S, Shangguan J, et al. Bifunctional ZnO-MgO/activated carbon adsorbents boost H2S room temperature adsorption and catalytic oxidation. Applied Catalysis B: Environmental. 2020;266:118674.
[58] Rodrigues AE, Zuping L, Loureiro JM. Residence time distribution of inert and linearly adsorbed species in a fixed bed containing "large-pore" supports: applications in separation engineering. Chemical Engineering Science. 1991;46:2765-73.
[59] Santos O, Nylander T, Paulsson M, Trägårdh C. Whey protein adsorption onto steel surfaces—effect of temperature, flow rate, residence time and aggregation. Journal of Food Engineering. 2006;74:468-83.
[60] Bak C-u, Lim C-J, Lee J-G, Kim Y-D, Kim W-S. Removal of sulfur compounds and siloxanes by physical and chemical sorption. Separation and Purification Technology. 2019;209:542-9.
[61] Ozekmekci M, Salkic G, Fellah MF. Use of zeolites for the removal of H2S: A mini-review. Fuel Processing Technology. 2015;139:49-60.
[62] Lee KX, Valla JA. Adsorptive desulfurization of liquid hydrocarbons using zeolite-based sorbents: a comprehensive review. Reaction Chemistry & Engineering. 2019;4:1357-86.
[63] Lee S-K, Jang Y-N, Bae I-K, Chae S-C, Ryu K-W, Kim J-K. Adsorption of Toxic Gases on Iron-Incorporated Na-A Zeolites Synthesized from Melting Slag. MATERIALS TRANSACTIONS. 2009;50:2476-83.
[64] Alonso-Vicario A, Ochoa-Gómez JR, Gil-Río S, Gómez-Jiménez-Aberasturi O, Ramírez-López CA, Torrecilla-Soria J, et al. Purification and upgrading of biogas by pressure swing adsorption on synthetic and natural zeolites. Microporous and Mesoporous Materials. 2010;134:100-7.
[65] Micoli L, Bagnasco G, Turco M. H2S removal from biogas for fuelling MCFCs: New adsorbing materials. International Journal of Hydrogen Energy. 2014;39:1783-7.
[66] Long NQ, Vuong HT, Ha HKP, Kuniawan W, Hinode H, Baba T. Preparation, characterization and H2S adsorptive removal of ion-exchanged zeolite X. J ASEAN Eng J Part B. 2016;51:4-12.
[67] Chen X, Shen B, Sun H, zhan G. Ion-exchange modified zeolites X for selective adsorption desulfurization from Claus tail gas: Experimental and computational investigations. Microporous and Mesoporous Materials. 2018;261:227-36.
[68] Liu X, Wang R. Effective removal of hydrogen sulfide using 4A molecular sieve zeolite synthesized from attapulgite. Journal of Hazardous Materials. 2017;326:157-64.
[69] Liu C, Zhang R, Wei S, Wang J, Liu Y, Li M, et al. Selective removal of H2S from biogas using a regenerable hybrid TiO2/zeolite composite. Fuel. 2015;157:183-90.
[70] Abdullah AH, Mat R, Somderam S, Abd Aziz AS, Mohamed A. Hydrogen sulfide adsorption by zinc oxide-impregnated zeolite (synthesized from Malaysian kaolin) for biogas desulfurization. Journal of Industrial and Engineering Chemistry. 2018;65:334-42.
[71] Rezaei S, Tavana A, Sawada JA, Wu L, Junaid ASM, Kuznicki SM. Novel Copper-Exchanged Titanosilicate Adsorbent for Low Temperature H2S Removal. Industrial & Engineering Chemistry Research. 2012;51:12430-4.
[72] Rezaei S, Jarligo MOD, Wu L, Kuznicki SM. Breakthrough performances of metal-exchanged nanotitanate ETS-2 adsorbents for room temperature desulfurization. Chemical Engineering Science. 2015;123:444-9.
[73] Alothman ZA. A review: Fundamental aspects of silicate mesoporous materials. Materials. 2012;5:2874-902.

[74] Wu S-H, Mou C-Y, Lin H-P. Synthesis of mesoporous silica nanoparticles. Chemical Society Reviews. 2013;42:3862-75.
[75] Dhage P, Samokhvalov A, Repala D, Duin EC, Tatarchuk BJ. Regenerable Fe–Mn–ZnO/SiO2 sorbents for room temperature removal of H2S from fuel reformates: performance, active sites, Operando studies. Physical Chemistry Chemical Physics. 2011;13:2179-87.
[76] Hussain M, Abbas N, Fino D, Russo N. Novel mesoporous silica supported ZnO adsorbents for the desulphurization of biogas at low temperatures. Chemical Engineering Journal. 2012;188:222-32.
[77] Xue Q, Liu Y. Removal of minor concentration of H2S on MDEA-modified SBA-15 for gas purification. Journal of Industrial and Engineering Chemistry. 2012;18:169-73.
[78] Chu X, Cheng Z, Zhao Y, Xu J, Zhong H, Zhang W, et al. Study on Sorption Behaviors of H2S by Triethanolamine-Modified Mesoporous Molecular Sieve SBA-15. Industrial & Engineering Chemistry Research. 2012;51:4407-13.
[79] Montes D, Tocuyo E, González E, Rodríguez D, Solano R, Atencio R, et al. Reactive H2S chemisorption on mesoporous silica molecular sieve-supported CuO or ZnO. Microporous and Mesoporous Materials. 2013;168:111-20.
[80] Babaei M, Anbia M. Novel Amine Modified Nanoporous SBA-15 Sorbent for the Removal of H2S from Gas Streams in the Presence of CH4 (RESEARCH NOTE) %J International Journal of Engineering. 2014;27:1697-704.
[81] Yoosuk B, Wongsanga T, Prasassarakich P. CO2 and H2S binary sorption on polyamine modified fumed silica. Fuel. 2016;168:47-53.
[82] Li L, Sun TH, Shu CH, Zhang HB. Low temperature H2S removal with 3-D structural mesoporous molecular sieves supported ZnO from gas stream. Journal of Hazardous Materials. 2016;311:142-50.
[83] Quan W, Wang X, Song C. Selective Removal of H2S from Biogas Using Solid Amine-Based “Molecular Basket” Sorbent. Energy & Fuels. 2017;31:9517-28.
[84] Okonkwo CN, Okolie C, Sujan A, Zhu G, Jones CW. Role of Amine Structure on Hydrogen Sulfide Capture from Dilute Gas Streams Using Solid Adsorbents. Energy & Fuels. 2018;32:6926-33.
[85] Saeedirad R, Taghvaei Ganjali S, Bazmi M, Rashidi A. Effective mesoporous silica-ZIF-8 nano-adsorbents for adsorptive desulfurization of gas stream. Journal of the Taiwan Institute of Chemical Engineers. 2018;82:10-22.
[86] Sigot L, Ducom G, Benadda B, Labouré C. Comparison of adsorbents for H2S and D4 removal for biogas conversion in a solid oxide fuel cell. Environmental Technology. 2016;37:86-95.
[87] Yang C, Yang S, Fan H-L, Wang J, Wang H, Shangguan J, et al. A sustainable design of ZnO-based adsorbent for robust H2S uptake and secondary utilization as hydrogenation catalyst. Chemical Engineering Journal. 2020;382:122892.
[88] Yang C, Wang J, Fan H, Hu Y, Shen J, Shangguan J, et al. Activated Carbon-Assisted Fabrication of Cost-Efficient ZnO/SiO2 Desulfurizer with Characteristic of High Loadings and High Dispersion. Energy & Fuels. 2018;32:6064-72.
[89] Yang C, Kou J, Fan H, Tian Z, Kong W, Shangguan J. Facile and Versatile Sol–Gel Strategy for the Preparation of a High-Loaded ZnO/SiO2 Adsorbent for Room-Temperature H2S Removal. Langmuir. 2019;35:7759-68.
[90] Wang X, Ma X, Sun L, Song C. A nanoporous polymeric sorbent for deep removal of H2S from gas mixtures for hydrogen purification. Green Chemistry. 2007;9:695-702.
[91] DeCoste JB, Peterson GW. Metal–Organic Frameworks for Air Purification of Toxic Chemicals. Chemical Reviews. 2014;114:5695-727.

[92] Barea E, Montoro C, Navarro JAR. Toxic gas removal – metal–organic frameworks for the capture and degradation of toxic gases and vapours. Chemical Society Reviews. 2014;43:5419-30.
[93] Vellingiri K, Deep A, Kim K-H. Metal–Organic Frameworks as a Potential Platform for Selective Treatment of Gaseous Sulfur Compounds. ACS Applied Materials & Interfaces. 2016;8:29835-57.
[94] Ahmed I, Jhung SH. Adsorptive desulfurization and denitrogenation using metal-organic frameworks. Journal of Hazardous Materials. 2016;301:259-76.
[95] Martínez-Ahumada E, López-Olvera A, Jancik V, Sánchez-Bautista JE, González-Zamora E, Martis V, et al. MOF Materials for the Capture of Highly Toxic H2S and SO2. Organometallics. 2020;39:883-915.
[96] Kenney WF, Eshaya AM. ADSORPTION OF XENON ON ACTIVATED CHARCOAL. ; Brookhaven National Lab., Upton, N.Y.; 1960. p. Medium: ED; Size: Pages: 21.
[97] Guo Y, Li Y, Zhu T, Ye M. Effects of Concentration and Adsorption Product on the Adsorption of SO2 and NO on Activated Carbon. Energy & Fuels. 2013;27:360-6.
[98] Balsamo M, Silvestre-Albero A, Silvestre-Albero J, Erto A, Rodríguez-Reinoso F, Lancia A. Assessment of CO2 Adsorption Capacity on Activated Carbons by a Combination of Batch and Dynamic Tests. Langmuir. 2014;30:5840-8.
[99] Alivand MS, Shafiei-Alavijeh M, Tehrani NHMH, Ghasemy E, Rashidi A, Fakhraie S. Facile and high-yield synthesis of improved MIL-101(Cr) metal-organic framework with exceptional CO2 and H2S uptake; the impact of excess ligand-cluster. Microporous and Mesoporous Materials. 2019;279:153-64.
[100] Allan PK, Wheatley PS, Aldous D, Mohideen MI, Tang C, Hriljac JA, et al. Metal–organic frameworks for the storage and delivery of biologically active hydrogen sulfide. Dalton Transactions. 2012;41:4060-6.
[101] Hamon L, Leclerc H, Ghoufi A, Oliviero L, Travert A, Lavalley J-C, et al. Molecular Insight into the Adsorption of H2S in the Flexible MIL-53(Cr) and Rigid MIL-47(V) MOFs: Infrared Spectroscopy Combined to Molecular Simulations. The Journal of Physical Chemistry C. 2011;115:2047-56.
[102] Hamon L, Serre C, Devic T, Loiseau T, Millange F, Férey G, et al. Comparative Study of Hydrogen Sulfide Adsorption in the MIL-53(Al, Cr, Fe), MIL-47(V), MIL-100(Cr), and MIL-101(Cr) Metal−Organic Frameworks at Room Temperature. Journal of the American Chemical Society. 2009;131:8775-7.
[103] Heymans N, Vaesen S, De Weireld G. A complete procedure for acidic gas separation by adsorption on MIL-53 (Al). Microporous and Mesoporous Materials. 2012;154:93-9.
[104] Jameh AA, Mohammadi T, Bakhtiari O, Mahdyarfar M. Synthesis and modification of Zeolitic Imidazolate Framework (ZIF-8) nanoparticles as highly efficient adsorbent for H2S and CO2 removal from natural gas. Journal of Environmental Chemical Engineering. 2019;7:103058.
[105] Kooti M, Pourreza A, Rashidi A. Preparation of MIL-101-nanoporous carbon as a new type of nanoadsorbent for H2S removal from gas stream. Journal of Natural Gas Science and Engineering. 2018;57:331-8.
[106] Mohideen MIH, Pillai RS, Adil K, Bhatt PM, Belmabkhout Y, Shkurenko A, et al. A Fine-Tuned MOF for Gas and Vapor Separation: A Multipurpose Adsorbent for Acid Gas Removal, Dehydration, and BTX Sieving. Chem. 2017;3:822-33.
[107] Sheikh Alivand M, Hossein Tehrani NHM, Shafiei-alavijeh M, Rashidi A, Kooti M, Pourreza A, et al. Synthesis of a modified HF-free MIL-101(Cr) nanoadsorbent with enhanced H2S/CH4, CO2/CH4, and CO2/N2 selectivity. Journal of Environmental Chemical Engineering. 2019;7:102946.

[108] Vaesen S, Guillerm V, Yang Q, Wiersum AD, Marszalek B, Gil B, et al. A robust amino-functionalized titanium(iv) based MOF for improved separation of acid gases. Chemical Communications. 2013;49:10082-4.
[109] Wang H, Zeng X, Wang W, Cao D. Selective capture of trace sulfur gas by porous covalent-organic materials. Chemical Engineering Science. 2015;135:373-80.
[110] Xu J, Xing W, Wang H, Xu W, Ding Q, Zhao L, et al. Monte Carlo simulation study of the halogenated MIL-47(V) frameworks: influence of functionalization on H2S adsorption and separation properties. Journal of Materials Science. 2016;51:2307-19.
[111] Zhou X, Su Z, Chen H, Xiao X, Qin Y, Yang L, et al. Capture of pure toxic gases through porous materials from molecular simulations. Molecular Physics. 2018;116:2095-107.
[112] Mi J, Liu F, Chen W, Chen X, Shen L, Cao Y, et al. Design of Efficient, Hierarchical Porous Polymers Endowed with Tunable Structural Base Sites for Direct Catalytic Elimination of COS and H2S. ACS Applied Materials & Interfaces. 2019;11:29950-9.
[113] Wang X-L, Fan H-L, Tian Z, He E-Y, Li Y, Shangguan J. Adsorptive removal of sulfur compounds using IRMOF-3 at ambient temperature. Applied Surface Science. 2014;289:107-13.
[114] Li Y, Wang L-J, Fan H-L, Shangguan J, Wang H, Mi J. Removal of Sulfur Compounds by a Copper-Based Metal Organic Framework under Ambient Conditions. Energy & Fuels. 2015;29:298-304.
[115] Bhoria N, Basina G, Pokhrel J, Kumar Reddy KS, Anastasiou S, Balasubramanian VV, et al. Functionalization effects on HKUST-1 and HKUST-1/graphene oxide hybrid adsorbents for hydrogen sulfide removal. Journal of Hazardous Materials. 2020;394:122565.
[116] Zhang H-Y, Zhang Z-R, Yang C, Ling L-X, Wang B-J, Fan H-L. A Computational Study of the Adsorptive Removal of H2S by MOF-199. Journal of Inorganic and Organometallic Polymers and Materials. 2018;28:694-701.
[117] Huang Y, Wang R. Highly selective separation of H2S and CO2 using a H2S-imprinted polymers loaded on a polyoxometalate@Zr-based metal–organic framework with a core–shell structure at ambient temperature. Journal of Materials Chemistry A. 2019;7:12105-14.
[118] Huang Z-H, Liu G, Kang F. Glucose-Promoted Zn-Based Metal–Organic Framework/Graphene Oxide Composites for Hydrogen Sulfide Removal. ACS Applied Materials & Interfaces. 2012;4:4942-7.
[119] Joshi JN, Zhu G, Lee JJ, Carter EA, Jones CW, Lively RP, et al. Probing Metal–Organic Framework Design for Adsorptive Natural Gas Purification. Langmuir. 2018;34:8443-50.
[120] Liu J, Wei Y, Li P, Zhao Y, Zou R. Selective H2S/CO2 Separation by Metal–Organic Frameworks Based on Chemical-Physical Adsorption. The Journal of Physical Chemistry C. 2017;121:13249-55.
[121] Zhang H-Y, Yang C, Geng Q, Fan H-L, Wang B-J, Wu M-M, et al. Adsorption of hydrogen sulfide by amine-functionalized metal organic framework (MOF-199): An experimental and simulation study. Applied Surface Science. 2019;497:143815.
[122] Belmabkhout Y, Bhatt PM, Adil K, Pillai RS, Cadiau A, Shkurenko A, et al. Natural gas upgrading using a fluorinated MOF with tuned H2S and CO2 adsorption selectivity. Nature Energy. 2018;3:1059-66.
[123] Bhatt PM, Belmabkhout Y, Assen AH, Weseliński ŁJ, Jiang H, Cadiau A, et al. Isoreticular rare earth fcu-MOFs for the selective removal of H2S from CO2 containing gases. Chemical Engineering Journal. 2017;324:392-6.
[124] Díaz-Ramírez ML, Sánchez-González E, Álvarez JR, González-Martínez GA, Horike S, Kadota K, et al. Partially fluorinated MIL-101(Cr): from a miniscule structure modification to a huge chemical environment transformation inspected by 129Xe NMR. Journal of Materials Chemistry A. 2019;7:15101-12.

[125] Sánchez-González E, Mileo PGM, Sagastuy-Breña M, Álvarez JR, Reynolds JE, Villarreal A, et al. Highly reversible sorption of H2S and CO2 by an environmentally friendly Mg-based MOF. Journal of Materials Chemistry A. 2018;6:16900-9.
[126] Zárate JA, Sánchez-González E, Jurado-Vázquez T, Gutiérrez-Alejandre A, González-Zamora E, Castillo I, et al. Outstanding reversible H2S capture by an Al(iii)-based MOF. Chemical Communications. 2019;55:3049-52.
[127] Gilliland ER, Baddour RF, Perkinson GP, Sladek KJ. Diffusion on Surfaces. I. Effect of Concentration on the Diffusivity of Physically Adsorbed Gases. Industrial & Engineering Chemistry Fundamentals. 1974;13:95-100.
[128] Sun S, Awadallah O, Cheng Z. Poisoning of Ni-Based anode for proton conducting SOFC by H2S, CO2, and H2O as fuel contaminants. Journal of Power Sources. 2018;378:255-63.
[129] Saadabadi SA, Thallam Thattai A, Fan L, Lindeboom REF, Spanjers H, Aravind PV. Solid Oxide Fuel Cells fuelled with biogas: Potential and constraints. Renewable Energy. 2019;134:194-214.
[130] Lanzini A, Madi H, Chiodo V, Papurello D, Maisano S, Santarelli M, et al. Dealing with fuel contaminants in biogas-fed solid oxide fuel cell (SOFC) and molten carbonate fuel cell (MCFC) plants: Degradation of catalytic and electro-catalytic active surfaces and related gas purification methods. Progress in Energy and Combustion Science. 2017;61:150-88.